January 2012

Effect of Platinum Particle Size on the Sulfur Deactivation of Hydrogenation

Lyndsey Michelle Baldyga
University of South Florida, lyndsey.baldyga@gmail.com

Effect of Platinum Particle Size on the Sulfur Deactivation of Hydrogenation Catalysts

by

Lyndsey Michelle Baldyga

A thesis submitted in partial fulfillment
of the requirements for the degree of
Master of Science in Chemical Engineering
Department of Chemical & Biomedical Engineering
College of Engineering
University of South Florida

Major Professor: John N. Kuhn, Ph.D.
Venkat R. Bhethanabotla, Ph.D.
Scott Campbell, Ph.D.

Date of Approval:
March 5, 2012

Keywords: Heterogeneous Catalysis, Noble Metal, Size Dependence, Colloid Chemistry, Sulfur Tolerance, Ethylene Hydrogenation

Acknowledgments

I would like to start by thanking my parents for providing me with financial support, via Florida Pre – Paid Program, for my undergraduate degree and emotional support during both of my degrees. My boyfriend, Austin Figler, was very supportive in my decision to get a graduate degree and was very patient during long days of writing and experimental work in the lab. Without the great leadership and advising of my thesis advisor, Dr. Kuhn, this thesis would have not been possible. My undergraduate advisor and thesis committee member, Dr. Campbell, was a great source of advice during both of my degrees in the department. Dr. Bhethanabotla, member of my thesis committee, has been a great source of advice during my graduate degree, and providing financial support, via an office job in the department. Without that job, I would have a lot more student loans and I cannot say enough how much that job meant to me. Finally, Dr. Yusuf Emirov was a great resource in using the TEM machine in the NREC. Last but not least, Robert Tufts and Luis Maldonado were a great help in the NREC.

Table Of Contents

List Of Tables

List Of Figures

List Of Equations

Abstract

A large concern of the fossil fuel and renewable energy industries is the sulfur poisoning of catalysts. In the case of noble metals, such as platinum, it is seen that there is a size trend associated with the level of activity in the presence of sulfur. Smaller nanoparticles could be more tolerant due to sulfur surface vacancies. On the other hand, larger particles could have less deactivation because the sulfur is more attracted to the smaller particles and the sulfur molecules bind stronger to these smaller particles.

The size effect of sulfur deactivation was investigated by testing four sizes of nanoparticles, ranging from 2 – 7 nm with and without sulfur by running an ethylene hydrogenation reaction. The synthesized particles were characterized by mass spectrometry, X – ray diffraction, and transmission electron microscopy. The 7 nm catalyst resulted in being the most sulfur tolerant due to the sulfur particles binding strongly to the smaller particles.

Chapter 1: Literature Review

1.1 Environmental Issues That Come From Fuel Processing

Transportation is an essential part of today's world. Fuel processing for transportation causes a variety of problems. The problem that is currently in the spotlight is the emission of harmful chemicals into the environment. These emissions include carbon dioxide (CO_2), methane (CH_4), nitrous oxides (NO_X), other hydrocarbons, sulfur, etc. In 2003, 27% of greenhouse gas emissions released into the environment could be attributed to the transportation industry. Greenhouse gases include, CO_2, NO_x, CH_4, and other hydrocarbons. Greenhouse gas emissions are expected to increase by 48% by 2025 from the 2003 numbers. The United States only accounts for 5% of the world's population but yet, this country produces around 21% of the world's greenhouse gas emissions. (U.S. Environmental Protection Agency Office of Transportation and Air Quality).

Greenhouse gas emissions are not the only type of harmful gas emitted into the atmosphere from fuel processing, sulfur dioxide is another harmful gas. In 2009, sulfur in fuel was one of largest forms of air pollution worldwide (Zhanghuai, Lv and Lv). Emissions of sulfur dioxide has been attributed to many environmental and health problems (Environmental Protection Agency). Sulfur dioxide, SO_2, emissions have decreased over the years due to strict regulations in place by the Environmental Protection Agency (EPA).

Harm of the air emissions is only one problem when using and processing fuel. Fuel processing and usage also causes damage to land and consumes a large volume of water. Due to the inadequate amount of drinkable water available, this is a high priority issue for the transportation industry to solve (Annenberg Learner).

Fresh water is a finite resource and every year 3000 km^3 of fresh water is used that cannot be regenerated by natural means. This loss is due to various uses, including the transportation industry (Sufiyanov, Katalymov and Gol'berg). The Texas Water Development Board has estimated that between 2010 and 2060, Texas's water supply would fall 18% and during this time the amount of people in the state would continue to increase. This would result in less water for an increased population (Annenberg Learner).

The transportation industry consumes a large amount of water and also contaminates large amounts of water. The amount of wastewater each year that is dumped into lakes, streams, etc. is about $5*10^8$ m^3 each year.

There are five different types of wastewater that come from transportation industry. These types of wastewater include, contaminated and not cleaned, inadequately treated, pure with no treatment, treated, and mixed water from domestic and production sources. Of the five different types of waste water, mixed waste water is the most polluted. Fuel processing not only affects the air we breathe, but another life source, the water we drink (Sufiyanov, Katalymov and Gol'berg).

1.2 Harm Of Sulfur Emissions

Sulfur emissions harm the environment and also harm human health. Air pollution caused by sulfur emissions causes acid rain, haze, and mercury methylation. Acid rain occurs all over the world and in some areas where this rain falls, it can be one hundred times more acidic than normal precipitation. Even though high concentrations of sulfur emissions are limited to certain cities, these emissions will spread to cities where the sources of these emissions are much less prominent. Sulfur emissions also cause haze and mercury methylation (Environmental Protection Agency). Mercury methylation causes a variety of health problems. For example, in unborn children mercury methylation can cause central nervous system damage. (Harvi Velasquez).

In addition the issues mentioned above, there are been many cases of early death due to asthma and bronchitis. These afflictions were related to high levels of sulfur in the body (Environmental Protection Agency). Also,

breathing high concentrations of sulfur have been linked to a decline in IQ, hearing loss, cancer, and cardiovascular disease. (Environmental Protection Agency).

Acid rain has its own environmental and human effects. Acid rain causes bodies of water to become more acidic than they normally would be. This results in a lower hydrogen concentration (pH) than aquatic animals and plants can survive. Visibility can also be decreased by the acid rain still in the air that has not yet condensed and fallen. Acid rain will increase the rate that certain materials and paint decay. (Environmental Protection Agency).

As seen above, sulfur emissions also cause haze (Harvi Velasquez). Haze occurs when sunlight tries to shine through tiny particles in the air. These tiny particles are pollutants in the air. Clarity of the air is reduced when there are more pollutants in the air. (Environmental Protection Agency). Haze causes the same health problems in people as acid rain causes. In the eastern United States, the normal visibility is between 15 – 30 miles. If there were no air pollution, this range would be 45 – 90 miles. This change would increase visibility by 200%. Removing more sulfur from fuel will results in less sulfur emissions thus reducing the harm to human health and the environment (Environmental Protection Agency).

Sulfur emissions have been on the decline since 1998 (Environmental Protection Agency). As of December 1, 2010 the amount of sulfur allowed in diesel fuel is 15 ppm for transportation vehicles, this value may vary in some states (Shell). In gasoline, the current regulation is 30 ppm. Although, many

air quality agencies are urging the EPA to reduce this concentration to 10 ppm. If the concentration of sulfur is reduced to this level, air pollution would decrease "as if 33 million cars and light trucks were no longer used" (Environment News Service). Regulations continue to get stricter to lessen the harm on human health and the environment. Also, sulfur content must be decreased to meet regulations for new technology. For example, fuel cells require sulfur level below 0.1 ppm, so sulfur will have to be reduced more to meet this standard, and to use fuel cell technology in vehicles (Sun).

Sulfur is also present in biomass feed stocks. This means that even if a switch is made to a renewable source of energy the sulfur will still need to be removed in order to meet environmental standards. The level of sulfur in biomass, before any processing, ranges from 50 – 230 ppm by volume.

Along with all the sulfur issues mentioned above, sulfur causes pipeline corrosions, thus reducing the life of a process plant. This can cause expensive pipeline removal and replacement. Also, the sulfur molecules poison the catalysts that are used in a reactor for sulfur removal. For this reason, a catalyst must be used that can still work under these conditions. One way to remove sulfur is hydrotreating, specifically hydrodesulfurization (Cheah, Carpenter and Magrini - Bair).

1.3 Hydrotreating

The sulfur in fuel can be removed by the use of an effective catalyst. A catalyst is used to begin a reaction or to increase the rate of an already occurring reaction (Bartholomew). One of the main goals of catalysis is to

form a catalyst that can form desired products instead of undesired products (Rioux, Song and Hoefelmeyer). The elimination of undesired products in a reaction is a very difficult process and requires extensive research. There are some catalysts that will work to remove sulfur from a process and some catalysts that will not work, despite being utilized for the same reasons in the same process (Bartholomew). The design of a catalyst usually includes "utilizing nanoscience to fabricate active catalyst sites, which are deposited on a support to produce a model heterogeneous catalyst" (Rioux, Song and Hoefelmeyer).

One way to remove sulfur is by hydrotreating. "Hydrotreating is the catalytic conversion and removal of organic sulfur, nitrogen, oxygen, and metals from petroleum crudes at high hydrogen pressures accompanied by hydrogenation of unsaturates and minor cracking of high molecular [weight] hydrocarbons" (Bartholomew). There are four different types of hydrotreating: hydrodesulfurization (HDS), hydrodenitrogenation (HDN), hydrodeoxygentation (HDO), and hydrometallization. The removal of sulfur is achieved by hydrodesulfurization (HDS). The reaction that is desired is seen below. This reaction states that the sulfur is removed from compound A and makes hydrogen sulfide, thus leaving compound "A" free of sulfur (Bartholomew).

$$H_2 + A - S \rightarrow H_2S + AH$$

Equation 1

1.4 Hydrodesulfurization (HDS)

HDS is a very important aspect of fuel refinery because sulfur is the most abundant heteroatom in fuel (Cattenot, Peeters and Geantet). The removal of sulfur is performed by HDS. The removal of sulfur will reduce the emissions and the harmful effects those emissions have. HDS can be performed in two ways, direct desulfurization (DDS) or hydrogenation (HYD).

In DDS, the "C – S bonds of the reactant molecule are broken by hydrogenolysis, leading to the formation of 3, 3' – dimethyl – biphenyl" (Rothlisberger). In the case of HYD, "the reactant molecule is first hydrogenated to intermediates, the C – S bonds of which are then broken to form 3, 3' dimethyl – cyclohexylbenzene and 3, 3' – dimethyl – bicyclohexyl" (Rothlisberger). A specific scheme of the pathways that HDS can take is seen below, in Figure 1. The molecule, 4, 6 – dimethyl – dibenzothiophene is of particular interest because the two methyl groups prevent sulfur from being on the surface, thus making the sulfur molecule harder to remove.

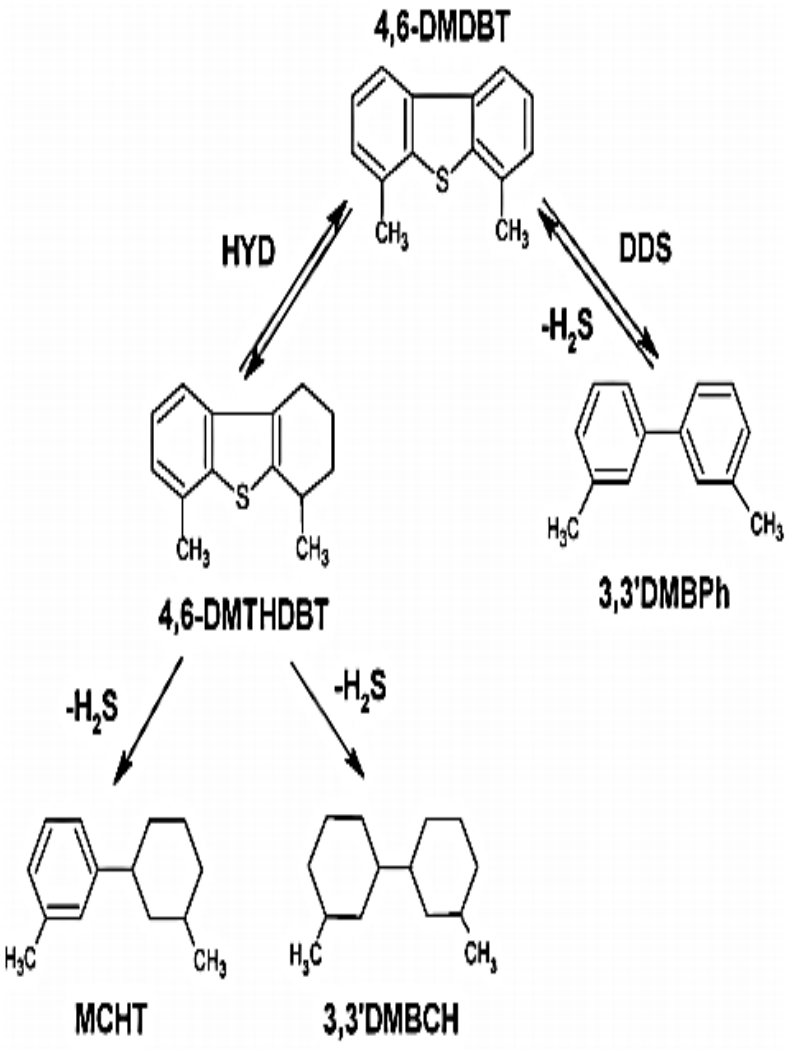

Figure 1. Pathways Of Hydrodesulfurization. Reprinted With Permission From Elsevier (Lewandowski, Da Costa and Benichou).

Figure 1 shows the two pathways that 4,6 – dimethyl – dibenzothiophene can take during HDS. When this molecule takes the hydrogenation route, the products formed are methylcarbonylhydrothiophene (MCHT) and 3,3’ dimethylbenzoalkane (DMBCH). When the molecule takes the DDS route, the product formed is only 3,3’ dimethylbenzophenol

(DMBPh). Depending on the products desired, a pathway will be chosen for HDS based on the type of catalyst that is used (Lewandowski, Da Costa and Benichou).

1.5 Why A New Catalyst Is Needed

Currently, there are a couple of different catalysts that are used for HDS, cobalt molybdenum (CoMo) supported on gamma – aluminum oxide (ϒ – Al_2O_3), nickel molybdenum (NiMo) supported on ϒ – Al_2O_3, and finally nickel tungsten (NiW) supported on ϒ – Al_2O_3. These catalysts are used "due to their high dispersion and high activity per unit volume, relatively low cost, tolerance to sulfur poisons, and high specific activities for removing oxygen - , nitrogen - , and sulfur – containing functional groups and/or heteroatoms" (Kuo and Tatarchuk). There has been little need to develop a new catalyst, but recently the need to process heavier crude oil is triggering a need for a better catalyst (Kuo and Tatarchuk). Also, in order to achieve the level of HDS needed for the ultra – low levels of sulfur, a new catalyst is needed for this new level of requirements (Pessayre, Geantet and Bacaud).

To reduce the sulfur level from 500 ppm to 50 ppm, a catalyst is needed that is four times more active than present catalysts (Knudsen, Cooper and Topsoe). To reduce the sulfur content further, an even more active catalyst will be needed (Rothlisberger). The conventional catalysts, such as CoMo, are usually used in the first stage of hydrotreating. After this initial hydrotreating, there are mainly dibenzothiophene derivatives seen in the feed. These derivatives do not respond to the normal catalysts used

because of the steric hindrances from the derivatives alkyl groups. Also, the hydrodenitrogenation must occur before the deep HDS can occur. When the nitrogen values are above 60 ppm it obstructs the deep HDS process (Lewandowski, Da Costa and Benichou).

The types of metals that have gained attention for use in this process come from the second and third rows of the periodic table. These metals include platinum, iridium, palladium, rhodium, and ruthenium. Noble metal sulfides have shown promising activity for the second step of HDS, deep HDS (Vit, Cinibulk and Gulkova).

1.6 Platinum As A Sulfur Tolerant Catalyst

Noble metal catalysts, such as platinum, are good options for catalysts to remove sulfur from fuel (Vit, Cinibulk and Gulkova). For example, fluid catalytic cracking (FCC) gasoline makes up 30 – 40% of the total gasoline produced. A sulfur tolerant catalyst is needed because the main components of FCC gasoline consist of thiols, sulfides, thiophene, and other sulfur compounds, around 85 – 95% (Brunet, Mey and Perot). Noble metal catalysts, such as Pt, "have a better hydrogenation performance than conventional metal sulfides in HDS, and may be used in the second reactor of a deep HDS process" (Sun). Platinum and palladium are less prone to be inactive in sulfur than other metals tested for deep HDS (Rothlisberger).

Platinum is a better catalyst to use, even though palladium is a cheaper material. In a study done by Niquille – Rothlisberger and Prins, Pt

was seen as a better desulfurization catalyst than Pd. Therefore, the Pt catalyst should be used as a sulfur removal tool (Niquille - Rothlisberger and Prins).

A proposed idea, mentioned in section 1.4, is to use a noble metal catalyst in the second reactor during two – stage deep HDS. Pt works best if the amount of sulfur entering the second reactor is low enough to keep good activity of the catalyst. If the sulfur level is too high, the activity of the catalyst will be lower and not worth the cost (Guo, Sun and Prins). The "strong metal sulfur chemisorption" of the catalyst causes the sulfur to poison the catalyst when in high concentration (Miller and Koningsberger).

As the catalyst is used the surface becomes saturated with sulfur atoms, this results the catalyst unusable due to catalyst deactivation (Miller and Koningsberger). At this time the catalyst will need to be regenerated. Catalyst deactivation means that there is a "decrease in catalytic activity and/or selectivity with time on stream" (Bartholomew).

There are a variety of different types of deactivation mechanisms that can occur. These deactivation mechanisms include coking, poisoning, sintering, contamination of catalyst, or physical catalyst changes. Coking of a catalyst occurs when there is adsorption of hydrocarbons onto the catalyst surface and solid carbon forms. Coking is usually a reversible process. In the case of coking, the catalyst can be regenerated by burning the hydrocarbons off of the catalyst surface. Sintering of a catalyst usually occurs at high temperatures. Sintering occurs when there is a "loss of catalytic surface area

due to crystallite growth in the catalytic phase [or] loss of support area due to support collapse and of catalytic surface area due to pore collapse on metal crystallites" (Bartholomew). When a catalyst is sintered it cannot be reversed. When the catalyst is physically changed, it is also irreversible. Contamination of a catalyst can also be reversible in certain cases.

When a catalyst becomes saturated with sulfur, as described above, the catalyst is poisoned. Poisoning of a catalyst occurs when a "strong chemisorption of reactants, products, or impurities on sites otherwise available for catalysis" (Bartholomew). Common poisons include oxygen, sulfur, phosphorous, mercury, tin, zinc, and carbon monoxide. The type of poison is usually indicative of the reaction being performed; sulfur poisoning is usually seen in hydrogenation, dehydrogenation, hydrocracking, oxidation of carbon monoxide and hydrocarbons, steam reforming of methane, naphtha, and CO hydrogenation of the syngas. Minimization of sulfur poisoning can be achieved by removal of impurities, changing the reaction conditions, and/or by adding substances that adsorb the poison.

Depending on the type sulfur poisoning that occurs, it may be an irreversible or reversible process. In the reversible case, the catalyst can be regenerated. Regeneration of a catalyst is performed to return the catalyst back to its original state. Regeneration of a sulfur poisoned catalyst is particularly difficult. One way to regenerate a sulfur poisoned catalyst is to run steam over the catalyst at 700^{o}C. In these conditions, 80% of sulfur was

removed from catalysts such as, "Mg – and Ca – promoted Ni steam reforming catalysts" (Bartholomew). For Pt catalysts, this is not considered an effective way to remove the sulfur.

Another way is to remove the sulfur is at very low oxygen partial pressures. This is a very slow process, but under these conditions regeneration is possible. After regeneration the Pt catalyst can be continued to be used. The regeneration process costs less than disposing of the old catalyst and purchasing a new catalyst (Bartholomew). Regeneration of the catalyst is a way of life when sulfur is used in the process. Two of the most important things for a sulfur removal process are a sulfur tolerant catalyst, and a way to regenerate the catalyst once it becomes poisoned (Bartholomew).

A study done by Lewandowski and et al. performs experiment on the HDS activity with tungsten carbide and tungsten trioxide both with platinum. For this experiment, the degree of HDS (%) was measured by Equation 2.

$$\boldsymbol{Degree\ of\ HDS}\ \ \% \ = \frac{\boldsymbol{S_H}}{\boldsymbol{S_S + S_{4,6DMDBT}}} * \mathbf{100},$$

Equation 2

S_s is the total products (molar percent) formed when the reaction with dimethyldibenzothiopene occurs. 4,6DMDT is the dimethyldibenzothiophene left after the reaction occurs (molar percent) and S_H is the amount (molar

percent) of the products that are not sulfur related. This equation will give the degree of HDS performed. The degree of HDS was then plotted against the contact time and W_2C – Pt was shown to have the highest degree of HDS activity for the same amount of contact time as W_2C and Pt – W_2C. This means that when the platinum is introduced after the synthesis of the W_2C the degree of HDS is better. When platinum is entered into the catalyst, after the initial synthesis of tungsten carbide, the catalyst was more sulfur tolerant. Also, when the contact time was increased it was seen that the performance was better when platinum was present. Contact time should be larger when platinum is involved because the results using the catalyst will be better than having a lower contact time (Lewandowski, Da Costa and Benichou).

Another study performed by W. R. A. M. Robinson et al. showed that at low sulfur concentrations noble metal catalysts worked the best. If the sulfur content of the fuel is high, a commercial catalyst will first need to be used to reduce the concentration of sulfur to a lower level because noble metal catalysts do not have a high sulfur resistance in high sulfur concentrations (Robinson, van Veen and de Beer).

Finally, although there is the option to combine platinum with many other metals to produce better properties. A study done by Merino, et al. showed that a monometallic noble metal catalysts, such as Pt, has the strongest catalytic active sites for HDS and HYD reactions. They are more

active than those same noble metal catalysts combined with molybdenum sulfide because monometallic catalysts have stronger active sites in the presence of sulfur (Merino, Centeno and Giraldo).

1.7 Catalyst Support Choice For Sulfur Removal

When choosing a support it is important to look at the sulfur tolerance properties of the support, but also to look at the other compounds that will be present and make sure the catalyst will not lose activity due to these compounds (Matsui, Masaru and Makoto). The support used on a catalyst can also have an effect on the activity during sulfur removal or the adsorption of sulfur onto the catalytic surface. One of the types of supports that have been studied is zeolites. Zeolites contain silicon, aluminum, and oxygen and they have a tetrahedral framework. These supports are very porous, which makes them good for use in heterogeneous catalysis (British Zeolite Association). Zeolites also reduce cracking activity, which in turn produces higher amounts of naphthalene and gasoline products. Although zeolites show good results, they are very expensive to use in production.

A study done by Fujikawa, et al. looked at an alternative of combining silica and alumina oxide and also alumina oxide by itself on platinum. The results of this study showed that the combined support was a better option than the alumina oxide support by itself (Fujikawa, Idei and Ebihara).

A catalyst resistant to sulfur can be increased when the catalyst is supported on an acidic zeolite support. Acidic zeolites are even great supports in high concentrations of sulfur. Acidic supports increase the sulfur

tolerance of a noble metal by electron transfer (Bihan and Yoshimura). An experiment was performed by Matsui, et al. and it was found that acidic USY zeolite was indeed a better support to use to increase sulfur tolerance than silica but this support was inhibited by the presence of nitrogen. This means that in an industrial setting that silica would be a better catalyst to use because although it is less sulfur tolerant than acidic zeolite it is not inhibited by the presence of nitrogen compounds, which is present in fuel (Matsui, Masaru and Makoto).

1.8 Adsorption Of Sulfur On Platinum

"Adsorption is the formation of chemical bonds between adsorbing species and an adsorbing surface driven by the propensity of adsorbent surface atoms to increase their coordination numbers" (Bartholomew). Adsorption occurs in two forms chemical, or chemisorptions, and physical, or physisorption. "Physisorption, is the relatively weak, nonselective condensation of gaseous molecules on a solid at relatively low temperatures; the attractive forces between adsorbate and adsorbent involve Van der Waals force, atomic distances typical of a Van der Waals layer, and heats of adsorption less than about 15 – 20 kJ/mol. Chemisorption, by contrast, is relatively strong, selective adsorption of chemically reactive gases on available sites of metal or metal oxide surfaces at relatively higher temperatures (i.e. 25 – 400^{o}C); the adsorbate – adsorbent interaction involves formation of chemical bonds and heats of chemisorption on the order of 50 – 300 kJ/mol" (Bartholomew).

The adsorption of sulfur on platinum usually occurs on the (111) plane. This plane is the most stable and usually is the most prevalent in small particles (Michaelides and Hu). The (111) plane is a lattice position; a lattice position is the "standard notation for a point in a crystallographic lattice". Other examples of lattice positions include, (110), (101), (001), etc. (Shackelford).

Chemisorption energy on Pt can be calculated by the following equation.

$$E_{ads} = E_A + E_{Pt} - E_{\frac{A}{Pt}}$$

Equation 3

E_A is the total energy of the adsorbate, E_{Pt} is Pt surface, and $E_{A/Pt}$ is the chemisorption system. Hydrogen adsorbs on Pt by binding to different sites, such as top, bridge, and face – centered – cubic (fcc). When sulfur adsorbs onto the Pt surface it adsorbs at the "fcc threefold hollow sites with an equilibrium S – Pt bond length of" 22.4 – 22.8 nm (Michaelides and Hu). The chemisorption energy was the highest at the fcc position and the lowest at the top position. The conclusion is that the fcc site is the most stable for the sulfur to chemisorbed onto the platinum. The following picture shows how hydrogen sulfide binds to Pt on three – fold, bridge, and top sites.

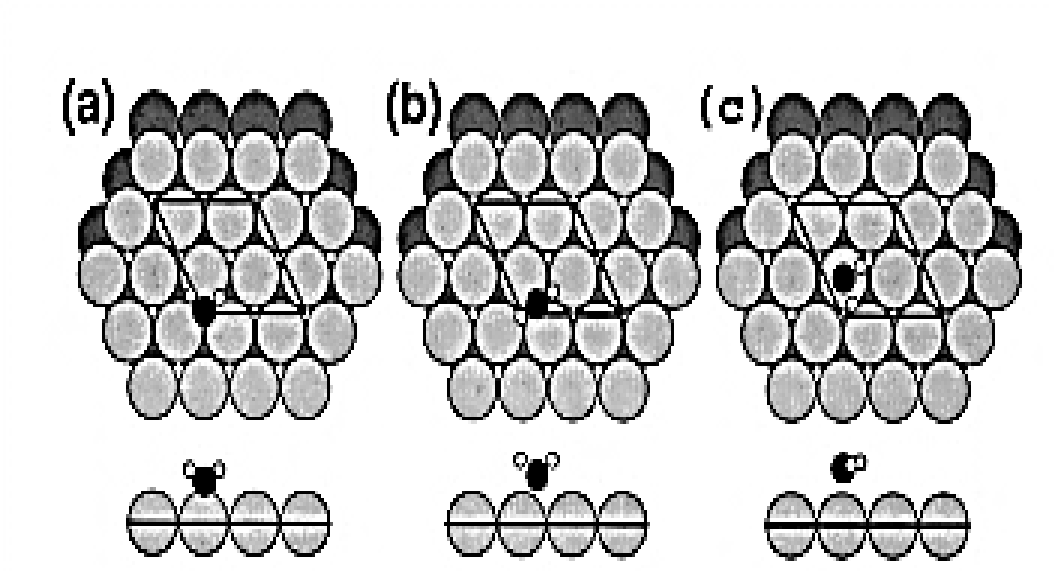

Figure 2. The Adsorption Of H_2S On Pt At Three – fold, Bridge, And Top Sites. Re – printed With Permission From American Institute Of Physics (Michaelides and Hu).

It was found that the top site on platinum has the highest bonding energy with hydrogen sulfide. Since sulfur adsorbs to the platinum (111) plane the most, and thus the most prevalent plane available for reaction, too much sulfur can result in an unusable catalyst (Michaelides and Hu).

1.9 Control The Size Of Pt Catalyst Using Polyvinylpyrrolidone (PVP)

To achieve the best results during HDS, the best catalyst must be used, including the size of the catalyst. The size dependence of sulfur tolerance on platinum catalysts is not a resolved issue and views on both sides of the spectrum have been presented. The Pt catalyst size can be changed by varying the amount of polyvinylpyrrolidone (PVP) and varying the amount of reductant (such as methanol) can achieve different sized Pt

catalysts. In a study done by Teranishi, catalysts from 19 – 50 Angstroms, 1.9 – 5.0 nm, were synthesized by the method described above. Teranishi found that "the particle size can be significantly controlled by the kind of alcohol and the amount of PVP at the high concentration of alcohol" (Teranishi, Hosoe and Tanaka). They also found that the size can be controlled by the amount of PVP in regards to Pt precursor in the solution.

Teranishi also describes stepwise growth. Stepwise growth is using an initial nanoparticle base, usually small in size, and growing the nanoparticles bigger by using the initial particles as a nucleus for each of the larger particles. Using the stepwise growth method with an alcohol that has a higher boiling point will result in nanoparticles that have a smaller distribution. This means that the nanoparticles will be true to size when tested and not a variety of largely distributed sizes. "Accurate control of the particle size is most important [when investigating] those novel physical and chemical properties" (Teranishi, Hosoe and Tanaka). If the catalyst size cannot be controlled, replication of experiments would be difficult. Therefore, PVP is used to keep this control for each experiment (Teranishi, Hosoe and Tanaka).

1.10 Best Pt Size For Sulfur Removal

It is a known fact that noble metals are active catalysts in the presence of sulfur, but the size dependence of this activity is unknown (Wang and Iglesia). There are different views on which size of platinum catalyst will be the most active in the presence of sulfur. It is important to vary the size

of particles during catalytic testing to achieve the optimum catalyst for the process. Either the smaller particles will be more active or the larger particles will be more active. Reinhoudt, et al. performed a study on platinum catalysts supported on amorphous silica alumina (ASA) from sizes of 1.2 – 4 nm and their activity was tested in the presence of sulfur. They found that the smaller particles were more active during the conversion of 4-ethyl, 6-methyldibenzothiophene (4-E,6MDBT) because the reaction still proceeds over sulfur vacancies that only the small platinum particles have (Reinhoudt, Troost and van Schalkwijk).

Another study was performed that had similar findings. The particle sizes that were studied ranged from 2 to 5 nm. The particles were then tested in the presence of sulfur and it was concluded that the smaller particles were more active in the presence of sulfur. They went on to explain that in the smaller particles "the residual noble metal phases coexist with the noble metal sulfur phases at the surface of the small Pt … particles" (Matsui, Masaru and Ichihashi). As the size increased it was seen that metal sulfur phases were only seen at the surface of the metal catalyst and no noble metal phases existed (Matsui, Masaru and Ichihashi). There is also the other view that believes the larger particles are more active in sulfur. In the case of ruthenium, another noble metal, a study was performed to observe the sulfur tolerance of different sizes of the metal catalysts. As a catalyst gets under the size of 10 nm, the coordination of the metal decreases with decreasing particle size and as coordination decreases intermediates of a reaction tend to bind more strongly to the particle. To see if this is true in the

presence of sulfur, Ru catalysts were supported on silica and the size ranged from 1.2 – 6.2 nm. These catalysts were studied for their sulfur tolerance by flowing thiophene over the catalysts and ranging the amount of H_2S from 0 – 10 kPa. Wang and Iglesia concluded that the turnover rates increased as the particle size increased, which is consistent with the fact that the sulfur would bind more strongly to particles that had lower coordination. Also, there are less sulfur vacancies seen on the smaller particles, which would allow for less activity in the presence of sulfur. Finally, smaller particles exhibit higher steady – state sulfur coverage" when exposed to sulfur (Wang and Iglesia).

Once this issue is resolved, the best size that is found can be applied to the formation of a bimetallic catalyst. It has been seen that the addition of palladium or rhodium can enhance the sulfur resistance of a platinum catalyst on aluminum oxide, this also a conflicting topic as seen in section 1.5. Further research can be done to make use of the most active size of platinum catalyst and apply it to a truly sulfur tolerant catalyst (Qian, Yoda and Hirai).

Chapter 2: Procedure

2.1 Pt Particle (2 nm) Synthesis

The smallest Pt nanoparticles were synthesized using a reflux setup with a round bottom flask in an oil bath. Sodium hydroxide (NaOH), 250 mg, (Sigma Aldrich reagent grade) was dissolved, by sonication: VWR B35ODA – DTH, in 12.5 mL of ethylene glycol (Sigma Aldrich reagent grade). This solution was combined with a solution of 12.5 mL of ethylene glycol and 0.25 g of chloroplatinic acid hexahydrate (H_2PtCl_6 * $6H_2O$), Sigma Aldrich 50% Pt basis. The resulting solution was added to a three-necked round bottom flask. The left and right necks were topped with septa and the middle neck was used in the reflux setup. The left neck contained an argon bubbling needle which was used to remove the dissolved oxygen in the solution while refluxing. The solution was heated at 155^{o}C for three hours.

After this time, the solution was cooled and then neutralized with a volume of 1 mL of 2M hydrochloric acid (HCl). Immediately after this, 12.2 mg of polyvinylpyrrolidone (PVP, Sigma Aldrich molecular weight 40,000 g/mol), dispersed in ethanol, was added to retain the size of the particles. The resulting amount of particle solution was 25 mL.

To wash these particles, 1 mL of particle solution was added to 9 mL of acetone, reagent grade from Sigma – Aldrich, and centrifuged, Clinical 100 VWR, for 20 minutes at 5000 rpm. This resulted in a black precipitate at the bottom of the vial. A pipette was used to remove the supernatant. To the black precipitate, 3 mL of ethanol was added. To the resulting ethanol/ particle solution, 9 ml of a mixture of hexane isomers, Sigma Aldrich, was added and centrifuged for 10 minutes at 3000 rpm. After centrifuging, the supernatant was removed and 3 mL of ethanol was added. This is repeated two more times (Kuhn, Huang and Chia - Kuang). The solution is now ready to be prepared for characterization and reaction experiments.

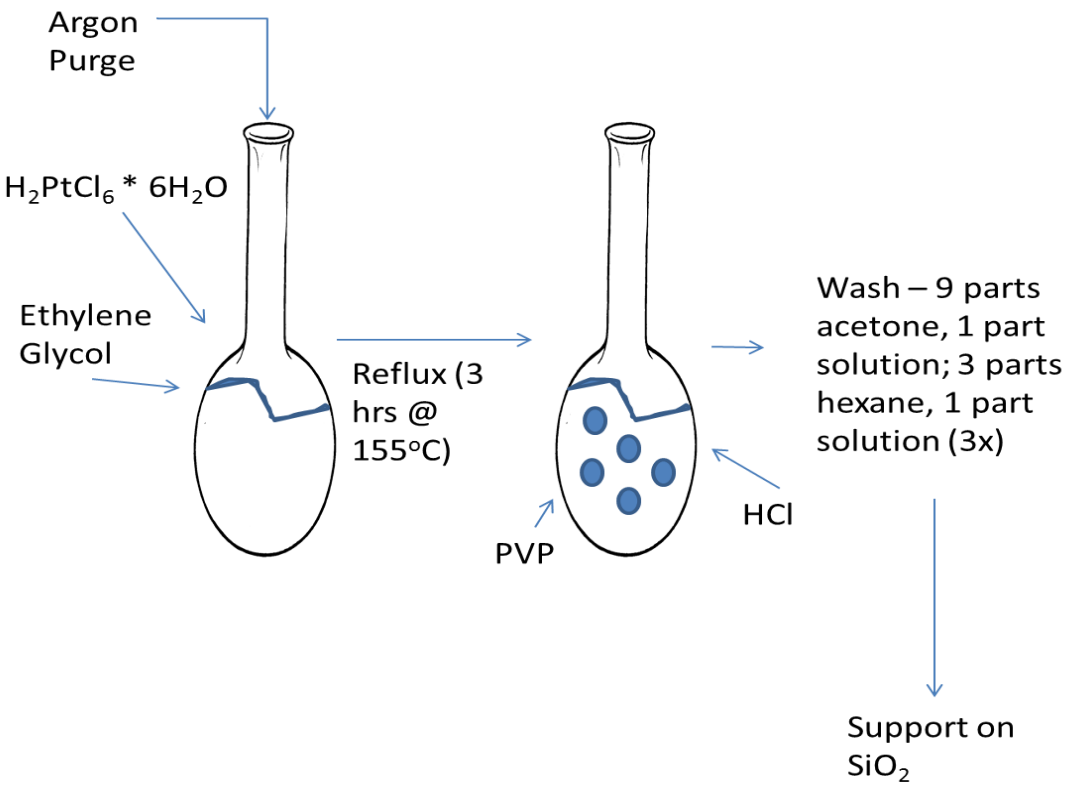

Figure 3. Scheme Of 2 nm Synthesis

2.2 Pt Particle (3.4, 4.3, And 6.8 nm) Syntheses

The three larger sizes of platinum nanoparticles were prepared in a reflux setup with a round bottom flask. Seeded growth was used to produce the 4.3 and 6.8 nm particles, with the 3.4 nm particles used as the seed. To make 3.4 nm particles, 62.9 mg H_2PtCl_6 was dissolved in 20 mL of distilled water. Next, 180 mL of methanol was then added to a round bottom flask. The water-H_2PtCl_6 solution was added to the methanol. Before starting the reflux, 133 mg of PVP (molecular weight 40,000 g/mol) was added to the mixture. A reflux set up with an oil bath was then set up. Parafilm was put around the connection between the condenser and the round bottom flask. The mixture was refluxed for three hours at 110^{o}C. During this time, the mixture turned a dark brown color.

Once the 3 hours were completed, the mixture was transferred to a beaker for the evaporation of methanol. The hot plate was set to 55^{o}C until the methanol was evaporated and only solid black platinum particles remained. These particles were re – dispersed in a minimum amount of ethanol. Once in ethanol, the particles were washed. The washing procedure follows the one for the smallest particles; except these particles do not need the initial acetone wash. This mixture was centrifuge for 10 minutes at 3000 rpm. After each separation, the particles were re-dispersed in ethanol, even after the last wash (Kuhn, Huang and Chia - Kuang). The particles are then prepared for TEM and XRD characterization. These 3.4 nm particles were used as a seed for the growth of the 4.3 nm (Kuhn, Huang and Chia - Kuang) and the 4.3 nm particles were used to seed the growth for the 6.8 nm

particles. To use these particles as a seed refers to adding more material and refluxing longer after the initial particles were synthesized. The difference between the syntheses was the amount of time the solution was refluxed and the concentration of PVP in the solution. A lower concentration of PVP allows for smaller particles. Also, when the precursor is added for the 4.3 and 6.8 nm particles, 10 mL of de – ionized water was used to dissolve the precursor (Kuhn, Huang and Chia - Kuang). Table 1 shows these differences. Figure 4 shows a scheme of the syntheses for the 3.4, 4.3, and 6.8 nm particles.

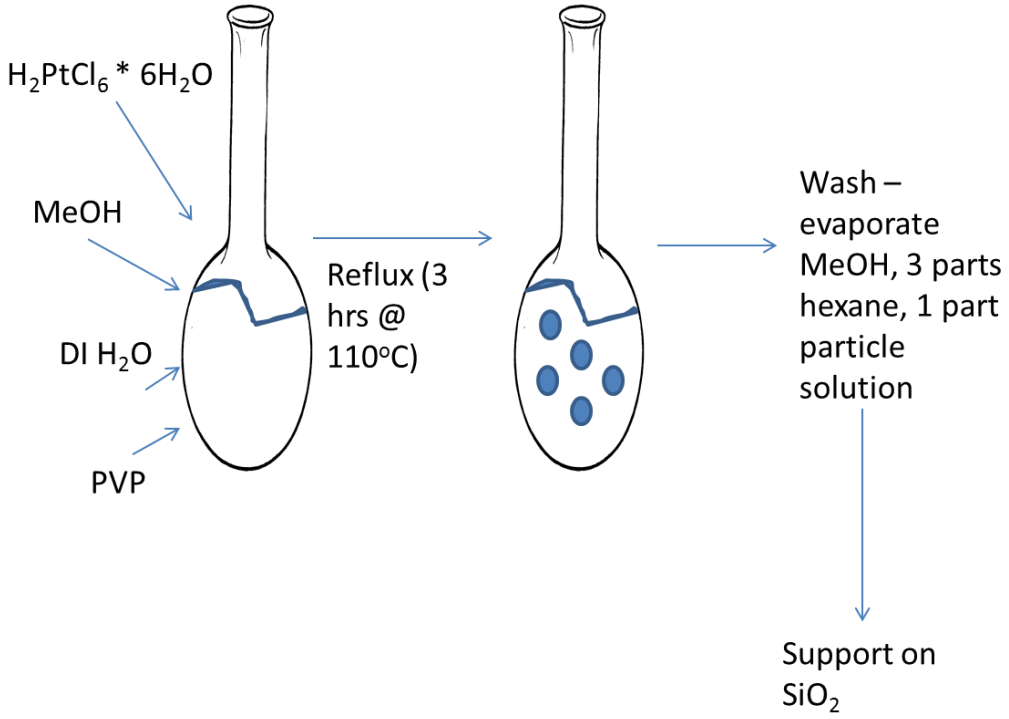

Figure 4. Scheme Of 3.4, 4.3, And 6.8 nm Syntheses

Table 1. Varying Precursor And Methanol Used

Particle Size (nm)	Methanol Added (mL)	Precursor Added (mg)	Total Time (hrs)
3.4	180	62.9	3
4.3	90	36.9	6
6.8	90	31.1	9

2.3 Immobilization On Silica

With the washed solution, the platinum particles were used to make one mass percent Pt on silica. The necessary amount of silica (CAB – O Silica ® M – 5 150 grade; surface area: 200 m^2/g) can be seen in Table 2. The large amount of silica used for the 2 nm particles is due to the increased amount of precursor used in the synthesis compared to the syntheses of the other particle sizes. Additional ethanol was added to these tubes to facilitate the mixing of the silica into the solution. The tubes were then sonicated for two hours in a 5.7 L VWR Ultrasonics Cleaner, model B3500A – DTH; 120 V; 60 Hz. The tubes were then centrifuged for 15 minutes at 5000 rpm. After centrifuging, the supernatant was removed leaving the supported particles behind. This solution was then dried in a LABCONCO Protector Laboratory Hood overnight. The next day the partially dried material was put into a VWR oven kept at 60^{o}C for another night (Kuhn, Huang and Chia - Kuang). The completely dried supported particles were ground into a fine powder using a

mortar and pestle. In addition to the samples seen above, an unwashed 2 nm Pt particle sample was supported on silica by following the procedure above. An unwashed sample means that is does not follow the washing procedure described in section 2.1 or 2.2, depending on the size of the particles.

Table 2. The Amount Of Silica Added To The Particle Solution

Catalyst Size (nm)	Amount of Silica added (mg)
2.0	24,750
3.4	2,300
4.3	3,705
6.8	4,919

Two mass percent Pt/silica was also made using the same procedure for the 3.4 nm particles only, one washed sample and one unwashed sample was made. For the washed sample, 1150 mg of silica, and for the unwashed, 574 mg of silica was used make two mass percent Pt/silica. The difference in the amount of silica used is due to the difference in amount of Pt particle solution used. The same procedure was used as to support the solution for two mass percent Pt/silica (Kuhn, Huang and Chia - Kuang).

2.4 Characterization

2.4.1 Transmission Electron Microscopy (TEM)

"The transmission electron microscope is in many ways analogous to a transmission optical microscope" (Brandon). Although there are a couple of differences, one being that the electron beam source is at the top and the recording system of the microscope is at the bottom. The other difference is that a transmission electron microscope the source is an electron beam. While in an optical microscope the source is light. The electron beam source is usually one of three types, heated tungsten filament, lanthanum hexaboride, and cerium hexaboride. Cerium hexaboride is the most recent addition to the types of electron beam sources. A transmission electron microscope can see samples as small as 0.1 nanometers.

This microscope is operated by "changing the lens [electron beam] current in order to adjust the focus length of the electromagnetic lens in order to focus a first image from the elastic scattered electrons that have been transmitted through the thin film specimen" (Brandon). "[T]he final image is [then] observed on a fluorescent screen that converts the high energy electron image into an image that is visible to the eye" (Brandon). On the screen, generally, the electron density is around 10^{-10} or 10^{-11} amperes/m^2. Some materials are damaged by the electron beam and this could cause the electron density to be lower in these types of samples. The microscope must also be kept under vacuum at all times because the

electron beam has a "limited path length in air" (Brandon). This vacuum needs to be at 10^{-7} torr for the highest resolution to be seen through the microscope (Brandon).

The atomic spacing and particle sizes were obtained using TEM. A small drop of well dispersed particles in ethanol was placed on 200 square mesh copper TEM grids with a formvar carbon film. The TEM grid was then used in FEI Tecnai TEM machine with an accelerating voltage of 200 kV, with the operation of the machine by Dr. Yusuf Emirov at the Nanotechnology Research and Education Center (NREC). The scale bars on the images obtained from TEM were 2 nm, 10 nm, and 20 nm for each size of the particles, at a magnification ranging from 750,000 times to 1 million times.

2.4.2 X – Ray Diffraction (XRD) – General And Alignment

An X – Ray diffractometer has three different parts, an X – ray source, X – Ray generator, and the diffractometer. The diffractometer portion of the X – ray diffractometer "controls the alignment of the beam, as well as position and orientation of both the specimen and the X – Ray detector" (Brandon). "The X - Rays are generated by accelerating a beam of electrons onto a pure metal target" (Brandon). These electrons then expel the ground – state electrons from the sample and then the X – Rays are discharged while re – filling the ground state electrons. The wavelength of the X – Rays produced is found by finding the frequency and dividing it by velocity of light ($3.8 * 10^{8}$ m/s). The X – ray wavelength produced is characteristic of the X – ray source being used.

The spectrum is generated by using a goniometer stage. This allows the sample to be moved over a variety of axes. Before the goniometer is used, alignment of the axes must be performed. Divergence slits are used in the diffractometer to allow for determination of the "area illuminated by the incident beam" (Brandon). The amount of area illuminated may need to be increased for known samples that the X – Ray spectrums seen are not in line with literature. X – Ray diffraction is a useful tool to see what is in the sample if you have a unknown mixture of materials that needs to be determined.

Confirmation of a platinum sample and the lattice plane can be obtained using XRD. A glass microscope slide was obtained and concentrated particles, for each size, in ethanol were dispersed in a large circle on the slide. This slide was dried over several days for use in the Philips X – Ray Diffractometer, in the NREC. The data was collected and aligned using Xpert Data Collector. Before beginning the experiment, the machine must be aligned according to the sample in the 2 – theta, Ω, and z directions. The fixed divergent slit and programmable receiving slit (PRS) were installed into the machine. These two pieces are used in general XRD experiments. For the aligning, on the incident beam side, a 0.1 copper attenuator, $\frac{1}{32}$ degree divergence slit, 0.04 radius soller slit was added. On the diffracted beam side, $\frac{1}{16}$ anti – scatter slit, nickel filter, and the PRS was set to 0.1 mm. A mask was also added to the incident beam optics but this size changes while

aligning, while the rest of the pieces in the machine will stay the same when aligning each sample. Finally, the power of the machine was turned up to 45,000 V and the current was turned up to 0.04 A.

To align 2 – theta, a manual scan is performed through 2 – theta with the following settings, range – 0.99 degrees, scan mode – continuous, time/step – 0.5 sec, step size – 0.01 degrees, and deg/sec – 0.02 deg/sec. Once the scan finished, a green line appeared, an alignment tool, and this line was moved to the peak maximum. Once the peak maximum is set this is the new alignment for 2 – theta for the duration of the experiment.

To align z, a manual scan through the z – axis was performed with the following settings, range – 1.99 mm, scan mode – continuous, time/step – 0.5 sec, and step size – 0.01 mm. Once the scan is finished, the green line was moved to half of the intensity seen during the scan.

To align omega, a manual scan through omega was performed with the following settings, range – 0.99, scan mode – continuous, time/step – 0.5 sec, step size – 0.01 degrees, deg/sec – 0.02 deg/sec. The green line was then moved to the maximum of the peak. Once the first omega alignment is complete, the z and omega must be done again to ensure proper alignment. For some samples, the z and omega will need to be aligned more than twice.

Table 3. Mask Size And Alignment Settings For The 6.8 nm XRD Sample

Sample Size (nm)	Mask Size (mm)	Alignment Settings		
		2θ (degrees)	Z (mm)	Ω (degrees)
6.8	20	-0.130	9.547	0.5958

2.4.3 XRD Experiments

For the actual experiment, ½ degree divergence slit, ½ anti – scatter slit, and the PRS was set to 0.3. The copper attenuator is removed once the experiment begins. A scan was performed in continuous mode and each setting change with particle size, time per step, step size, and the length of the experiment.

Table 4. The XRD Experiment Settings For Each Sample

Particle Size	Time/Step	Step Size	Length of Experiment
6.8 nm	7.5	0.18	1 hr 9 mins

2.4.4 Temperature – Programmed Experiments

Four temperature – programmed experiments were performed. Each sample for these experiments was 50 mg of supported, 2% Pt in silica, 3.4 nm particles. Two additional experiments were performed with 50 mg of 1%

Pt in silica, 2.0 nm particles. These experiments were performed with a mass spectrometer. Mass spectrometry "provides the molecular weight and valuable information about the molecular formula, using a very small sample" (L.G. Wade). In the mass spectrometer, the sample's molecules are broken apart or fragmented.

There are two different forms of mass spectrometry electron impact ionization and magnetic deflection. Electron impact ionization means that the sample is struck with an electron beam and the "positively charged fragments are detected by the mass spectrometer" (L.G. Wade). Magnetic deflection separates the ions by attracting the positive ions "to a negatively charged accelerator plate, which has a narrow slit to allow some of the ions to pass through" (L.G. Wade). In this case, the magnetic field can be changed so all the possible fragment masses can be seen. A graph is then produced with the m/z values on the x – axis and the abundance of each m/z value on the y –axis; m/z value means the mass of the ion over the ion's charge (L.G. Wade).

Magnetic deflection mass spectrometry was used for these experiments. Each catalyst was put into a U – tube reactor and insulation was added to simulate a packed bed reactor. Quartz wool was used as insulation in the U-tube reactor and around the reactor and a Thermo Scientific Thermolyne furnace was used to heat the sample in the reactor. Before each experiment, a pretreatment was performed by running helium gas at 50 standard cubic centimeters per minute (sccm) over the sample. To

allow for analysis the valve was also opened to the mass spectrometer. To flow the gases over the catalyst the valves above the reactor were opened. The filament status on the computer was then changed to the "on" position. The gauge pressure was then checked to be sure it was less than 1 atm. The temperature was taken up to 110^{o}C Celsius from 22^{o}C at 10^{o}C per minute and then held at 110^{o}C for one hour.

For the first experiment, 2% Pt in silica 3.4 nm washed sample and 5 sccm of oxygen gas was flowed over the sample after the valve was opened, and 45 sccm of helium gas were flowed over the sample. The temperature was taken from 42^{o}C to 600^{o}C at 10^{o}C per minute. Once the temperature reached 600^{o}C, the temperature was held for hour. For the experiment, the gases flow over the catalyst, react with the catalyst, and then enter the mass spectrometry equipment, Cirrus MKS mass spectrometer. The abundance of the fragments seen by the mass spectrometer is then recorded on the computer. This same experiment was also performed for an unwashed 3.4 nm sample of 2% Pt in silica. Two additional experiments were performed on 2 nm 1% Pt in silica. This is a temperature programmed oxidation (TPO) experiment.

For the fifth experiment, the same pre-treatment procedure was followed, the hydrogen gas valves were opened and then the gas was turned on to 5 sccm, and 45 sccm of helium gas was flowed over the sample while the temperature was taken from 45^{o}C to 600^{o}C at 10^{o}C per minute. Once the

temperature reached 600°C the temperature was held for one hour. The m/z values being looked at were the same as in the 10% oxygen in helium experiment. This is temperature programmed reduction (TPR).

For the sixth experiment, the same pre-treatment procedure was also followed, 50 sccm of helium gas was flowed over the sample while the temperature was increased from 50°C to 600°C at a rate of 10°C per minute. The temperature was held at 600°C for one hour. The time for the temperature to reach 600°C in each experiment was around one hour making the total experiment time about two hours in length. The m/z values being looked at were the same as in the previous two experiments. This is a baseline experiment.

2.5 Catalytic Experiments

The catalytic experiments were performed using gas chromatography for the sulfur experiments and for the non – sulfur experiments mass spectrometry was utilized. Two different machines were used to avoid sulfur poisoning of the non – sulfur experiments, as sulfur can build up in the pipes of the machine that is using sulfur. A gas chromatograph, Perkin – Elmer Autosystem I, is used by inserting a small amount of the sample, 1 microgram, into an injector. As the sample goes through the gas chromatography column the components are separated and leave the column at different times. As the components leave the column they can then enter the thermal conductivity detector (TCD) to be analyzed separately (L.G. Wade).

2.5.1 Ethylene Hydrogenation Without Sulfur

The amount of catalyst used in each U – tube reactor with the respective particle size can be seen in the Table 5 below. The mass spectrometer used for these experiments was the same mass spectrometer as the one used for the temperature programmed experiments above, Cirrus MKS Mass Spectrometer. Before starting the experiment, the catalyst was purged for 30 minutes with 50 sccm of helium. During the experiment and bypass, helium was set to flow at 51.2 sccm, hydrogen was set to flow at 25 sccm, and ethylene was set at 1.3 sccm. This totaled in 77.5 sccm of gas flow. The valves on each gas must be turned on before turning the gases on to prevent a buildup of pressure. These gases, at first, were not flowed over the catalyst. Instead a bypass was performed, at room temperature, to get a baseline for the experiment. Measurements were taken every five seconds.

Table 5. Amount Of Catalyst Used Without Sulfur

Catalyst Size (nm)	Amount of Catalyst used (mg)
2.0	1.7
3.4	2.2
4.3	4.2
6.8	6.1

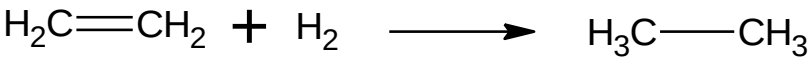

Figure 5. Reaction Without Sulfur

Once steady state is reached, the temperature on the furnace is set to 40°C with a ramp rate of 1°C/min. The gases are flown over the catalyst with the gas flowrate unchanging from the bypass portion of the experiment. The experiment is complete when the gases have reached steady state.

2.5.2 Ethylene Hydrogenation With Sulfur

To test the activity of the catalyst in the presence of sulfur, the catalyst was first pretreated with thiophene before beginning the experiment and after the purge. The purge lasted for 30 minutes while flowing 5 sccm of helium over the catalyst. Once the valve for the helium gas that bubbles the thiophene was turned on, the gas was set to 1 sccm. In addition, the helium gas not bubbling thiophene was set to 100 sccm, another helium gas was set to 50 sccm, and the hydrogen was set to 50 sccm. This amounted in a total gas flow of 201 sccm. The sulfidation pretreatment was performed at 150°C with a ramp rate of 10°C per minute and held at that temperature for thirty minutes. The amount of catalyst used in each experiment can be seen below in Table 6, this resulted in a total of four experiments with sulfur.

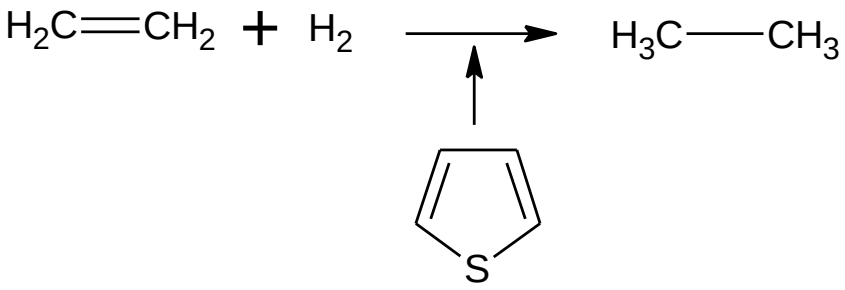

Figure 6. Ethylene Hydrogenation Reaction With Sulfur

Table 6. Amount Of Catalyst Used With Sulfur

Catalyst Size (nm)	Amount Of Catalyst Used (mg)
2.0	89.8
3.4	35.6
4.3	26.7
6.8	37.9

After the sulfidation procedure, the gas flow rates were set to the same flow rates as the non – sulfur experiments. The catalyst was first bypassed to get a baseline for the experiment. Once every 30 minutes, measurements were taken by a six – port valve and this valve has two positions, A and B. While the valve is in position B, the sample is flowing from the furnace and out through the vent. When a sample is ready to be taken, the valve is moved from position B to position A. When the valve is in position A, the sample gases flow from the reactor tube and fill the sample loop. Once 0.2 minutes have passed, the sample loop is sufficiently filled and

the valve is turned back to position B. Turning the valve back to position B pushes the sample contained in the sample loop into the gas chromatograph and the sample is then analyzed. Figure 7 shows this process in more detail. The sample is analyzed with the computer program Turbochrom Navigator. This bypass experiment was performed with each particle size.

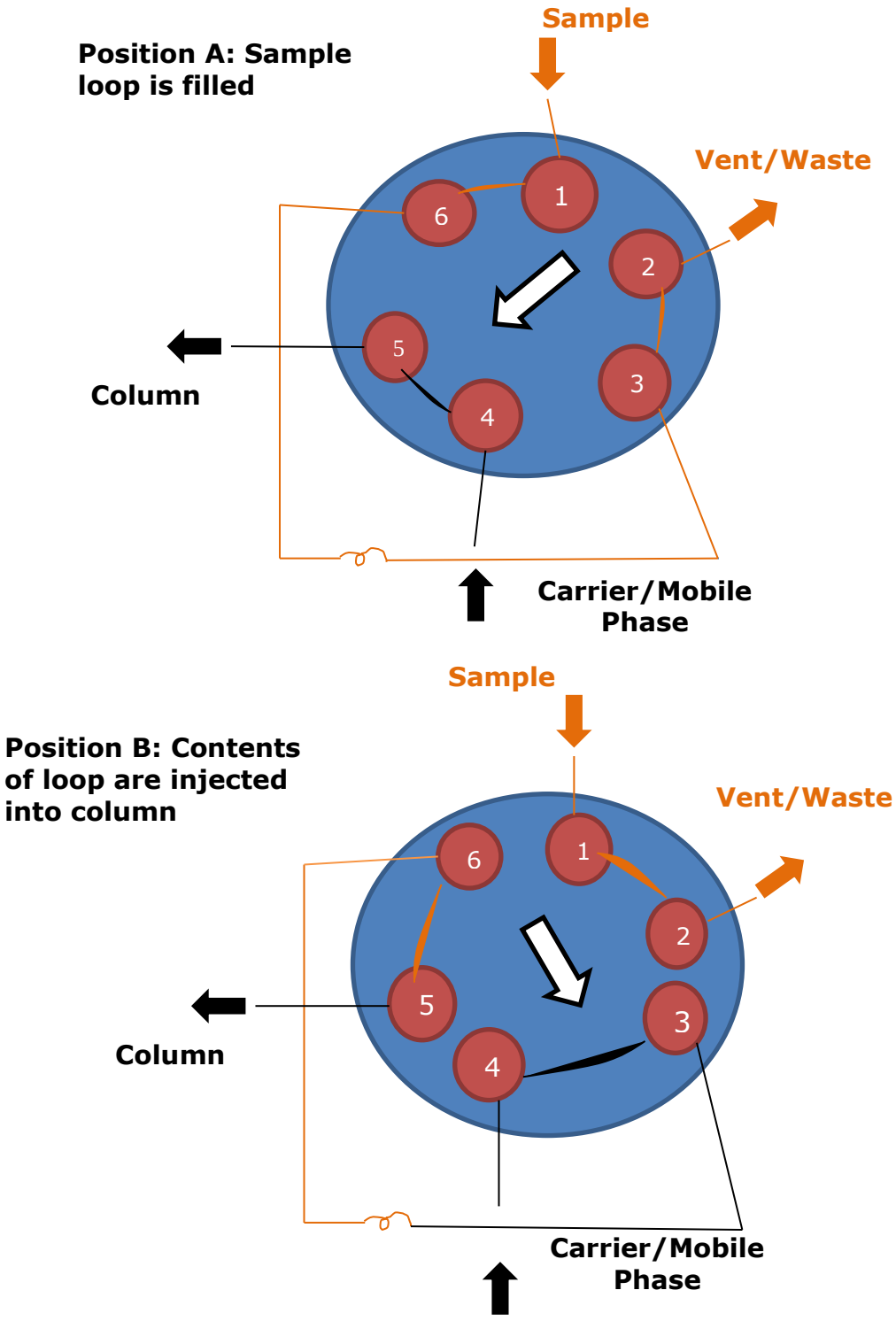

Figure 7. Diagram Of GC Valve System

After the bypass was completed, the gases were then flown over the catalyst, by opening the valves above the furnace, to perform the reaction with the platinum catalyst of each size. This results in a total of four experiments. Each experiment was performed at 40^{o}C with a ramp rate of 1^{o}C per minute. Measurements were taken about every 30 minutes until steady state was reached. This signified the end of the experiment.

Chapter 3: Results And Discussion

Chapter 3 will begin by explaining the results of the synthesis of the nanoparticles. This chapter will then end by describing and analyzing the results of the characterization, TEM and XRD, and the catalytic experiments.

3.1 TEM

3.1.1 Platinum Nanoparticle Results (2 nm)

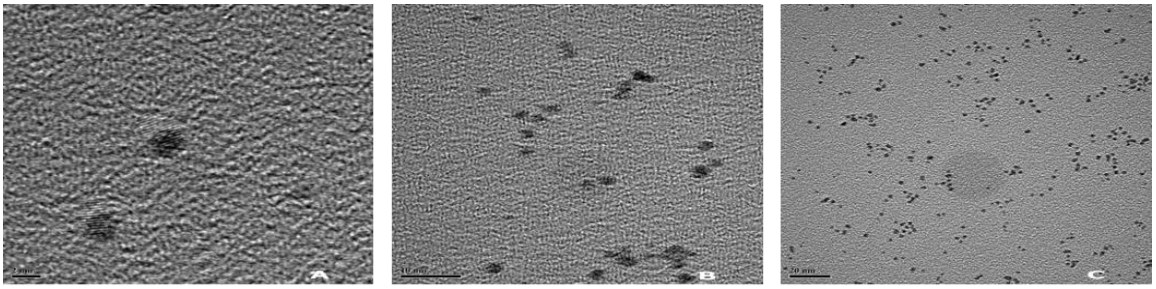

Figure 8. 2 nm Pt Particles TEM Images A: 2 nm Scale Bar, B: 10 nm Scale Bar, C: 20 nm Scale Bar

TEM experiments confirm the size of the particles seen in the microscope and the atomic spacing of the metal in the particles. The TEM images seen above in Figure 8 confirm the synthesis of spherical particles. With use of the program ImageJ, freeware from NIST, 100 particles were

sized using the scale bar as the reference. In Figure 9, the confirmation of platinum particles can be seen by measuring the atomic spacing of the particles. The atomic spacing is 2.3 Angstroms, (111) plane of platinum, all atomic spacing values reported from this section on was confirmed by the Xpert Highscore Program Database in USF's NREC.

The Xpert Highscore Program Database reported the Pt atomic spacing as around 2.25 Angstroms. This measurement confirms the presence of platinum. The atomic spacing for each metal is characteristic to that metal and thus the presence of platinum can be confirmed. The spacing between ten peaks was measured and then divided by ten, to get an average, to obtain the atomic spacing.

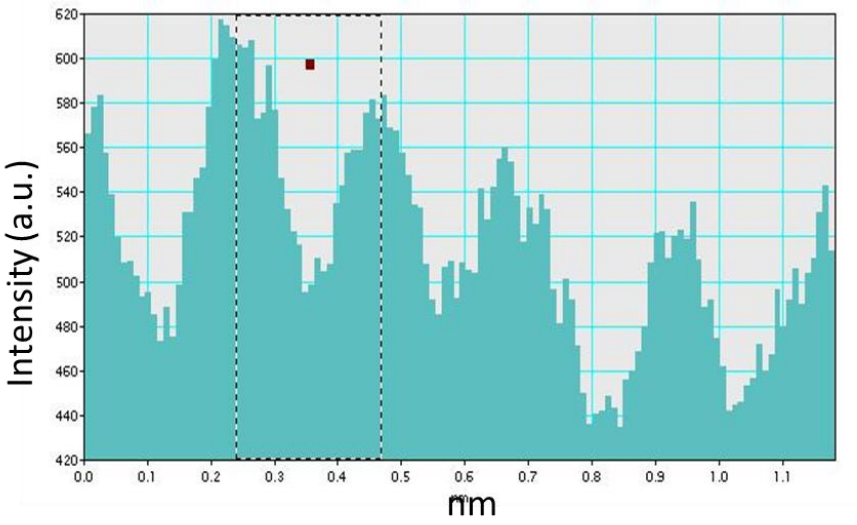

Figure 9. Atomic Spacing Of 2 nm Platinum Particles

The size distribution of the smallest particle size is seen in Figure 10a. The average size of the smallest particles is 2.0 nm with a standard deviation of 0.37 nm. The size distribution shows that the average size falls in the highest concentration of particles. One – third of the particles measured fall into the range of 1.89 – 2.15 nm. Particles measured fell in the range of 1.1 – 3.2 nm.

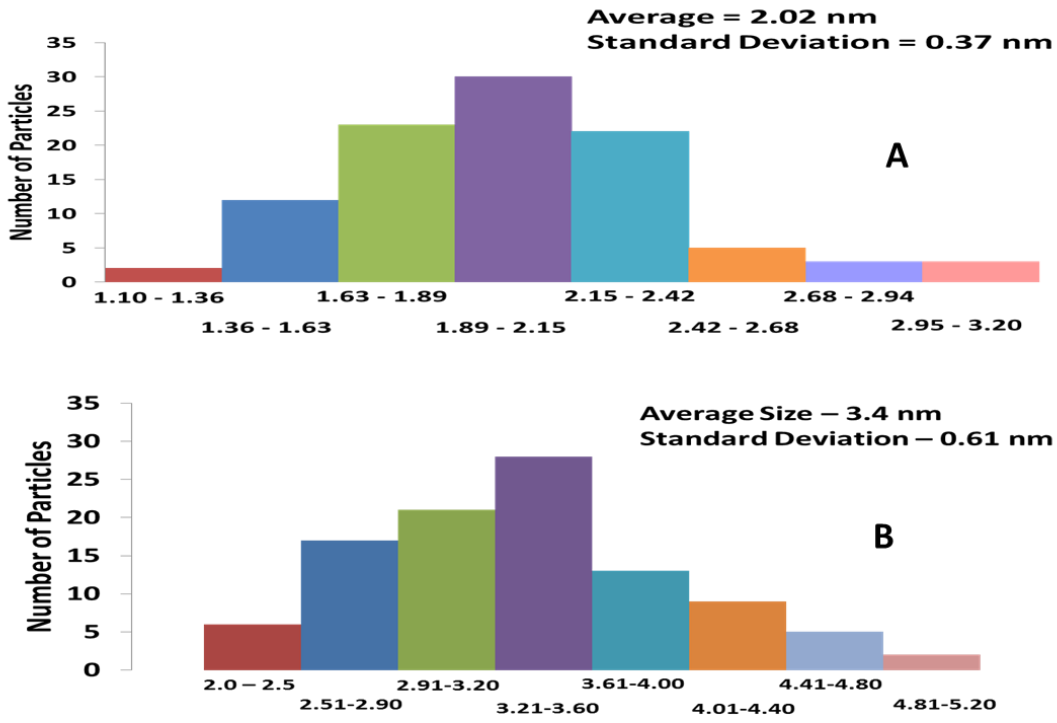

Figure 10. Size Distributions Of The Pt Particles - A: 2 nm, B: 3.4 nm

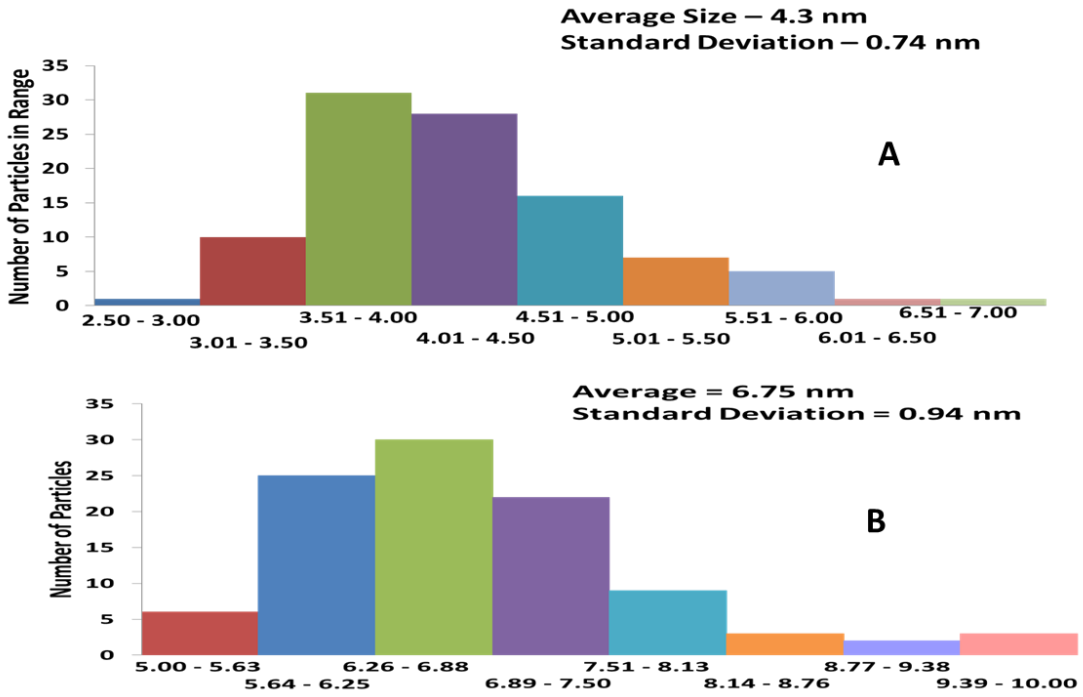

Figure 11. Size Distribution Of Pt Particles - A: 4.3 nm, B: 6.75 nm

3.1.2 Platinum Nanoparticle Results (3.4 nm Washed)

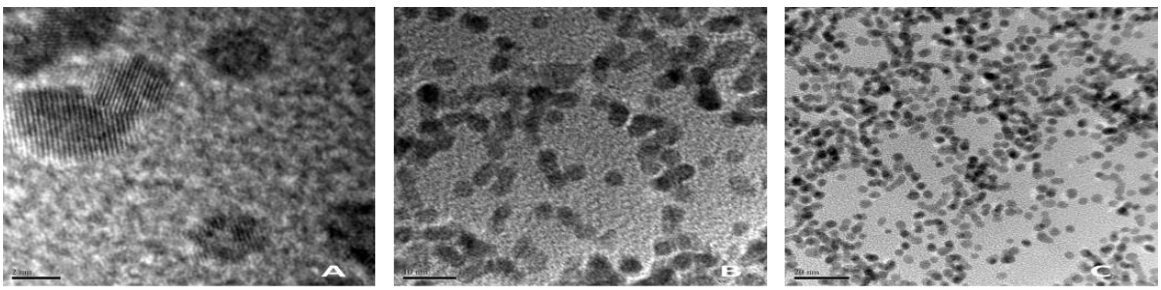

Figure 12. TEM Images Of 3.4 nm Pt Particles. A: 2 nm Scale Bar, B: 10 nm Scale Bar, C: 20 nm Scale Bar

Figure 12 shows the TEM images for the 3.4 nm Pt particle size. These images confirm the synthesis of spherical particles. Figure 10 – B shows the size distribution of the 3.4 nm particle size. The average size of the particles measured is 3.4 $\pm$ 0.61 nm. About one – third of the particles measured fall in the range, 3.21 – 3.6 nm, where the average size lies. The total range of particles measured from this synthesis is 2 nm – 5.2 nm. Below in Figure 13, the atomic spacing was measured to confirm the presence of platinum in the particles. The atomic spacing was 2.1 Angstroms, which is characteristic when platinum is present.

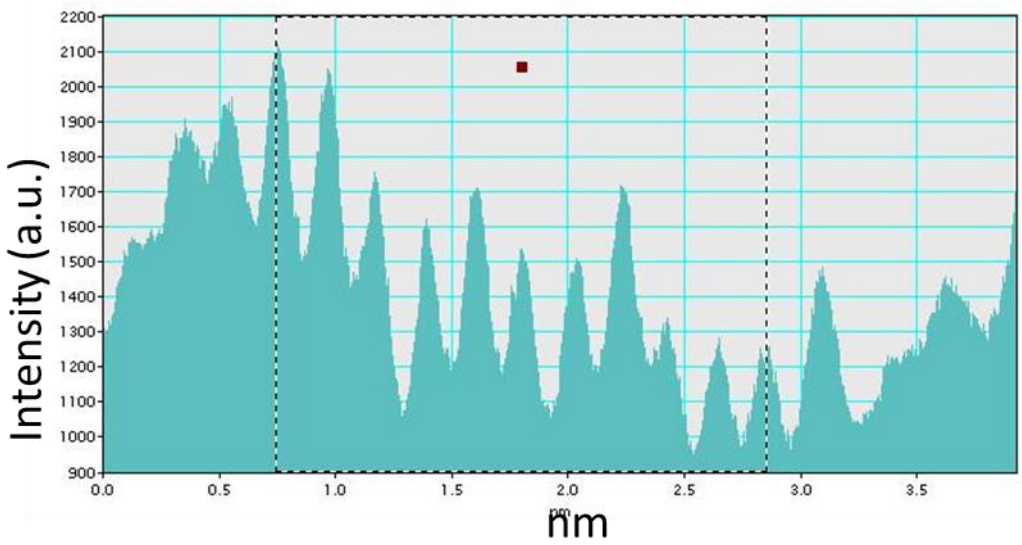

Figure 13. Atomic Spacing Of 3.4 nm Particles

3.1.3 Platinum Nanoparticle Results (3.3 nm Unwashed)

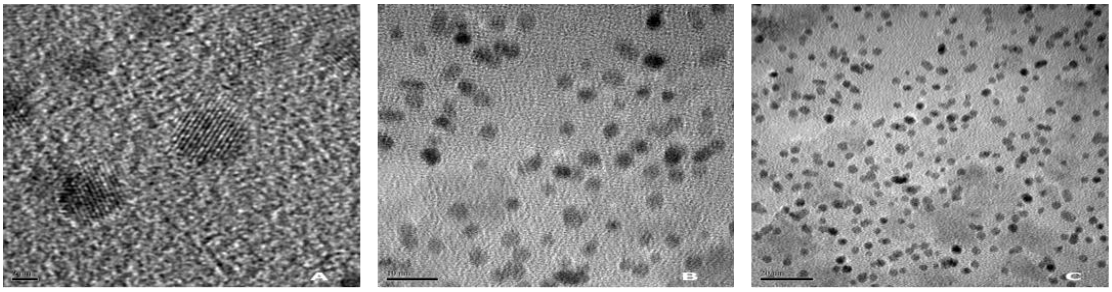

Figure 14. TEM Images Of 3.3 nm Pt Particles. A: 2 nm Scale Bar, B: 10 nm Scale Bar, C: 20 nm Scale Bar

Seen above in Figure 14, it is confirmed that spherical particles were formed during the synthesis of 3.3 nm Pt particles. Using the same method as the previous sizes observed, 100 particles were measured to find the size. Figure 15A shows the size distribution of the measured 100 particles. The average size of the unwashed Pt particles is 3.3 $\pm$ 0.74 nm. The range of the 3.3 nm Pt particle size is between 2.1 – 5.2 nm.

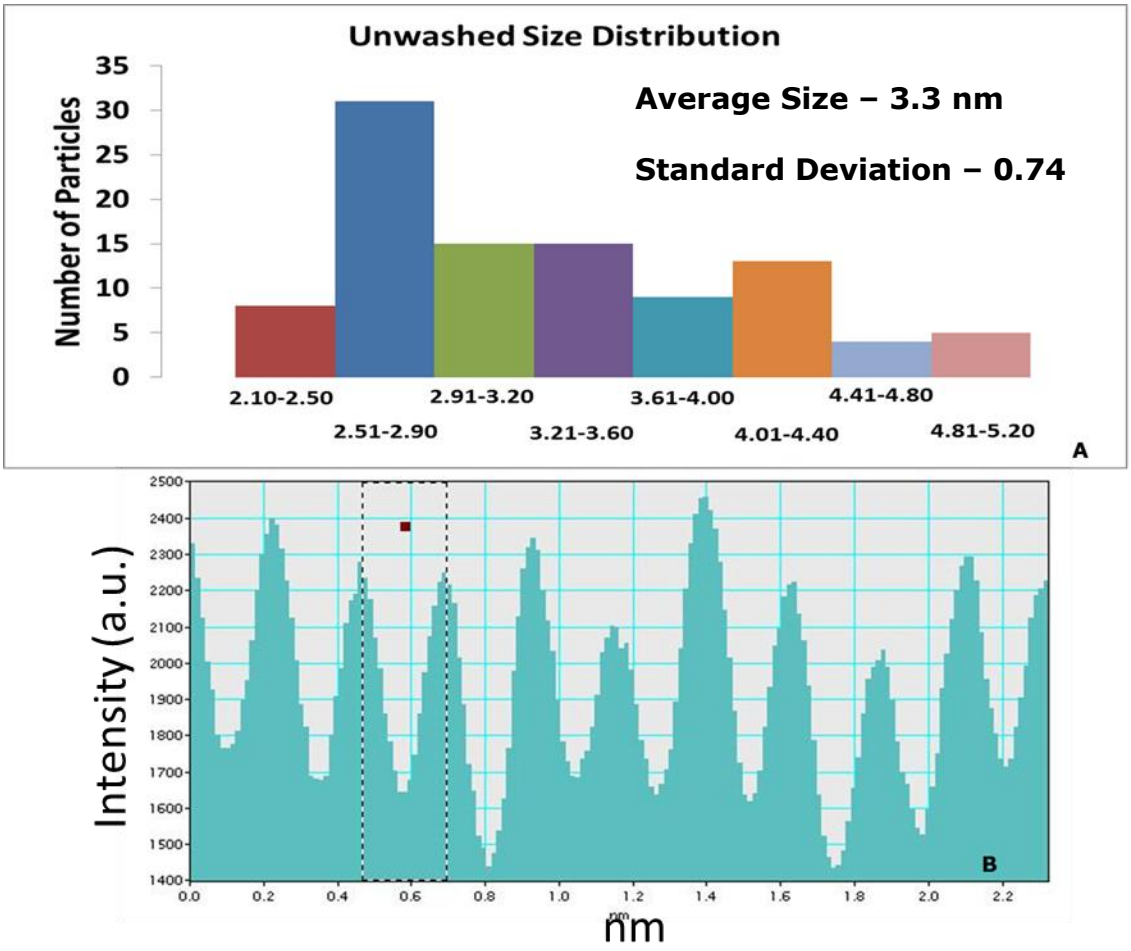

Figure 15. A: 3.3 nm Size Distribution, B: Atomic Spacing Of 3.3 nm Particles

Figure 15B shows the atomic spacing of the 3.3 nm unwashed Pt particle size. The atomic spacing was found to be 2.3 Angstroms, this length is characteristic of platinum and confirms the presence of Pt in this particle size. The unwashed 3.3 Pt particle size was synthesized to prove the effectiveness of the washing sequence. More information about this experiment can be seen in the temperature – programmed experiments section.

3.1.4 Platinum Nanoparticle Results (4.3 nm)

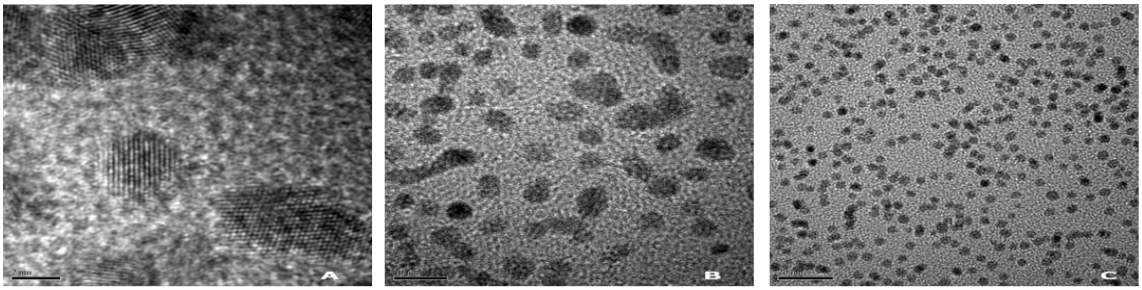

Figure 16. TEM Images Of 4.3 nm Pt Particles. A: 2 nm Scale Bar, B: 10 nm Scale Bar, C: 20 nm Scale Bar

The particles seen in Figure 16 represent the 4.3 nm particles at different magnifications. The pictures above confirm the synthesis of spherical nanoparticles and the measurement of this particle size is confirmed as an average of 4.3 nm. The standard deviation of this particle size is 0.74 nm. Figure 11A shows the size distribution of this 4.3 nm Pt particle size and the range of the particles measured is between 2.5 – 7 nm. About two – thirds of the particles measured fall in the range of 3.51 – 4.5 nm, where the average lies.

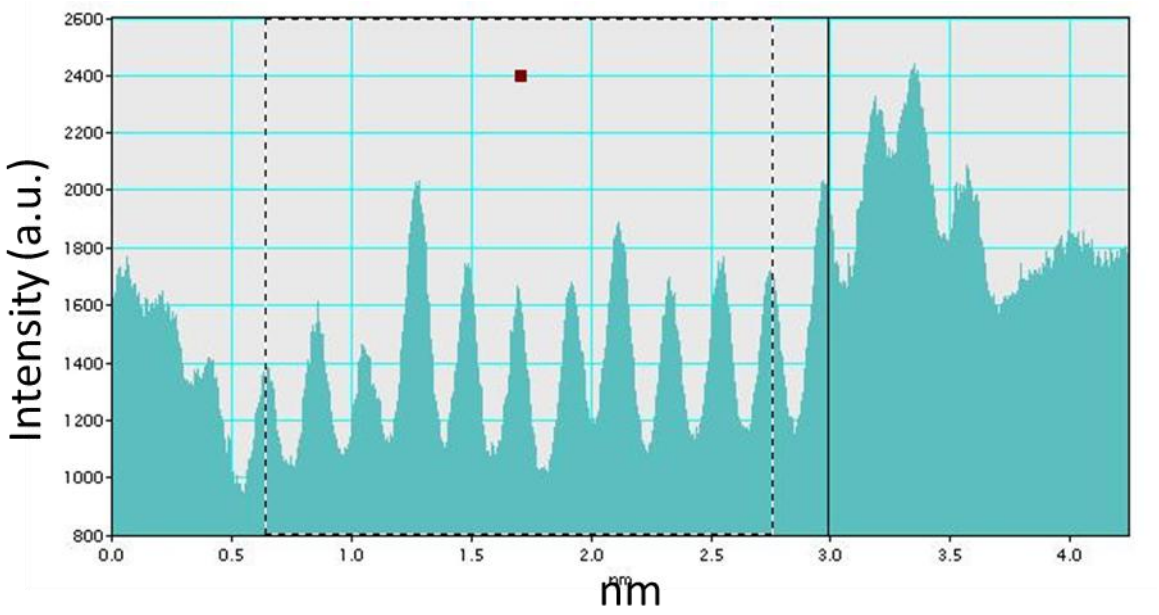

Figure 17. Atomic Spacing Of 4.3 nm Particles

Figure 17 shows the atomic spacing for one of the 4.3 nm Pt particle size. The atomic spacing of this particle size is 2.2 Angstroms, which is characteristic of platinum. An atomic spacing that is characteristic of platinum confirms that the particles seen in the TEM images in Figure 15 are platinum nanoparticles.

3.1.5 Platinum Nanoparticle Results (6.8 nm)

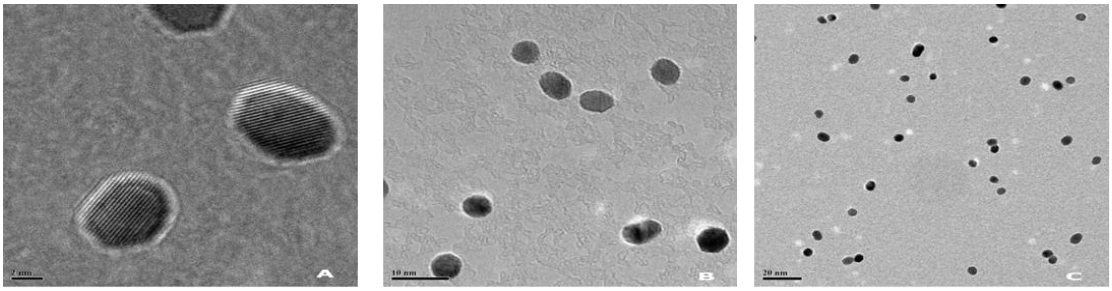

Figure 18. TEM Images Of 6.8 nm Pt Particles. A: 2 nm Scale Bar, B: 10 nm Scale Bar, C: 20 nm Scale Bar

TEM images of different magnifications seen in Figure 18 confirm the synthesis of spherical particles. Figure 11B shows the size distribution of the largest size of synthesized nanoparticles. The average size of the largest particle size is 6.8 nm with a standard deviation of 0.94 nm. The size of the particles ranged from 5 nm – 10 nm and one – third of the particles measured fell between 6.26 – 6.88 nm.

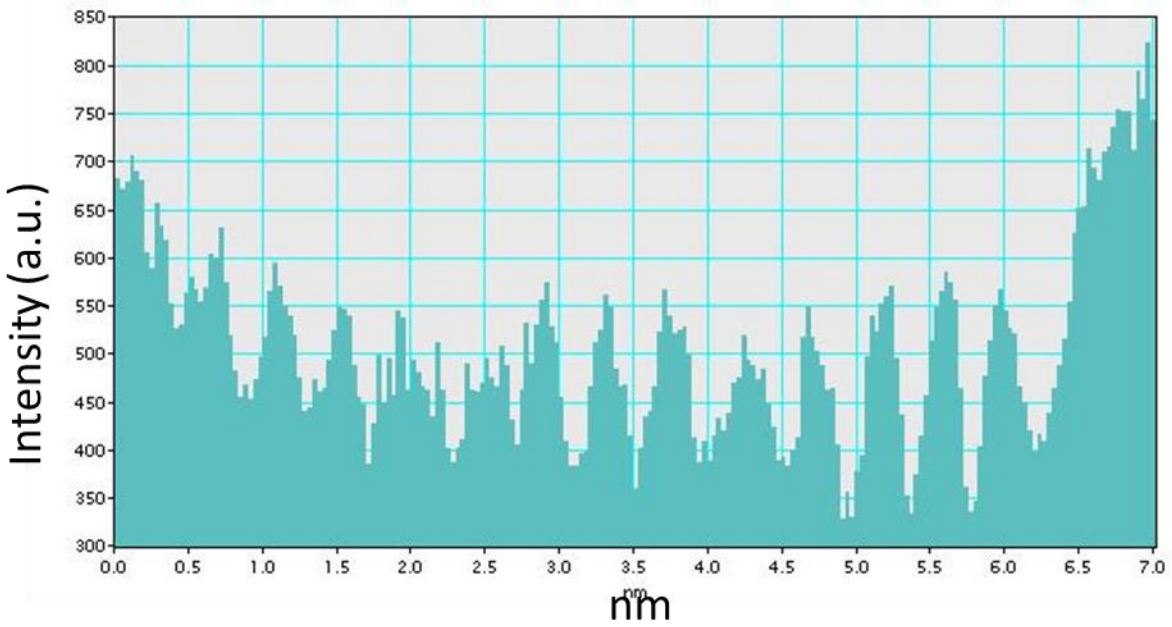

Figure 19. Atomic Spacing Of 6.8 nm Particles

The atomic spacing of a particle, Figure 19, was measured, by Yusuf Emirov, to be 2.3 Angstroms. This length is characteristic of platinum, which proves that platinum is present in this nanoparticle. Figure 19 shows the image which measures the size as well as the atomic spacing of a particle.

3.2 XRD Experiment (6.8 nm)

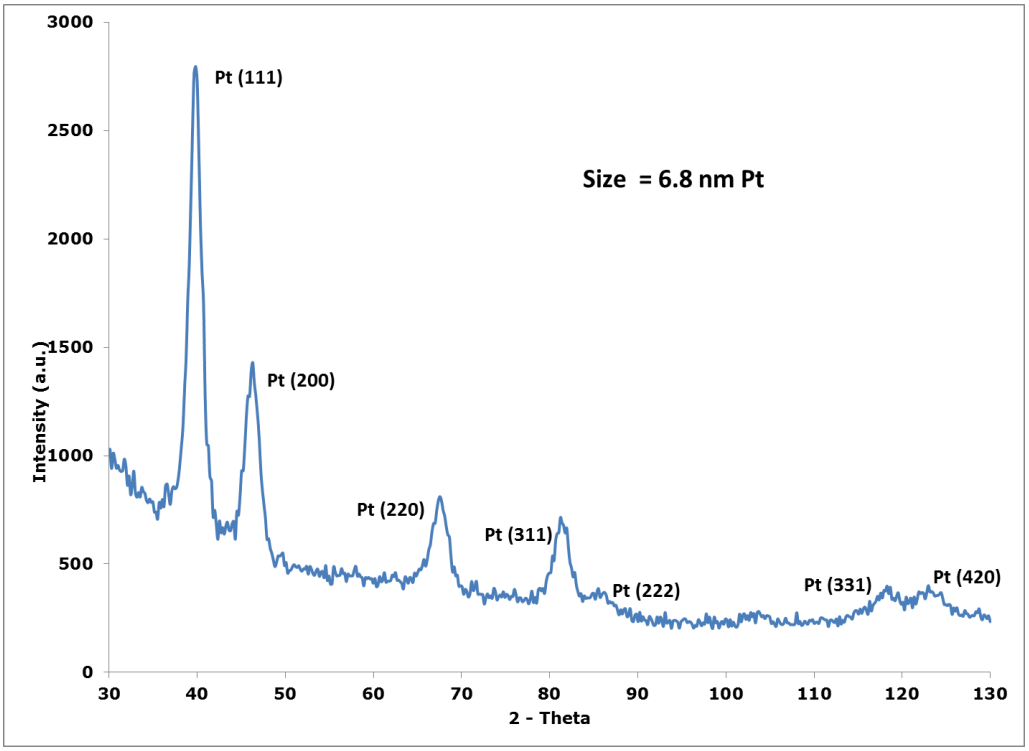

Figure 20. XRD Results Of 6.8 nm Pt Particle

An XRD experiment is compared spectrum to confirm the presence of certain metals in the particles being measured. Figure 20 shows the results of the 6.8 nm XRD experiment. This experiment was performed to prove the existence of Pt in the solution synthesized and find the crystallographic plane that is most prevalent (Brandon). The plane that is most prevalent is the plane with the most intense signal. Figure 20 shows that the (111) plane is the most prevalent. The signals shown in Figure 20 were compared to a reference pattern for Pt from the Xpert Highscore Database. The reference pattern matched fairly well with the pattern seen above.

3.3 Temperature – Programmed Experiments Results

Three different types of temperature – programmed experiments were performed, an inert, oxidation (10% oxygen in helium), and reduction (10% hydrogen in helium). Temperature – programmed experiments are performed to see the types of fragments that come off in different environments. These fragments and the temperatures the fragments are seen at are compared to the literature for consistency. Before these experiments were performed, the 3.4 nm washed particle size and the 3.3 nm unwashed particle size were supported on silica (2% Pt). After the particle sizes were supported and dried, they were ground into a fine powder for use in the mass spectrometer.

3.3.1 Temperature – Programmed Inert

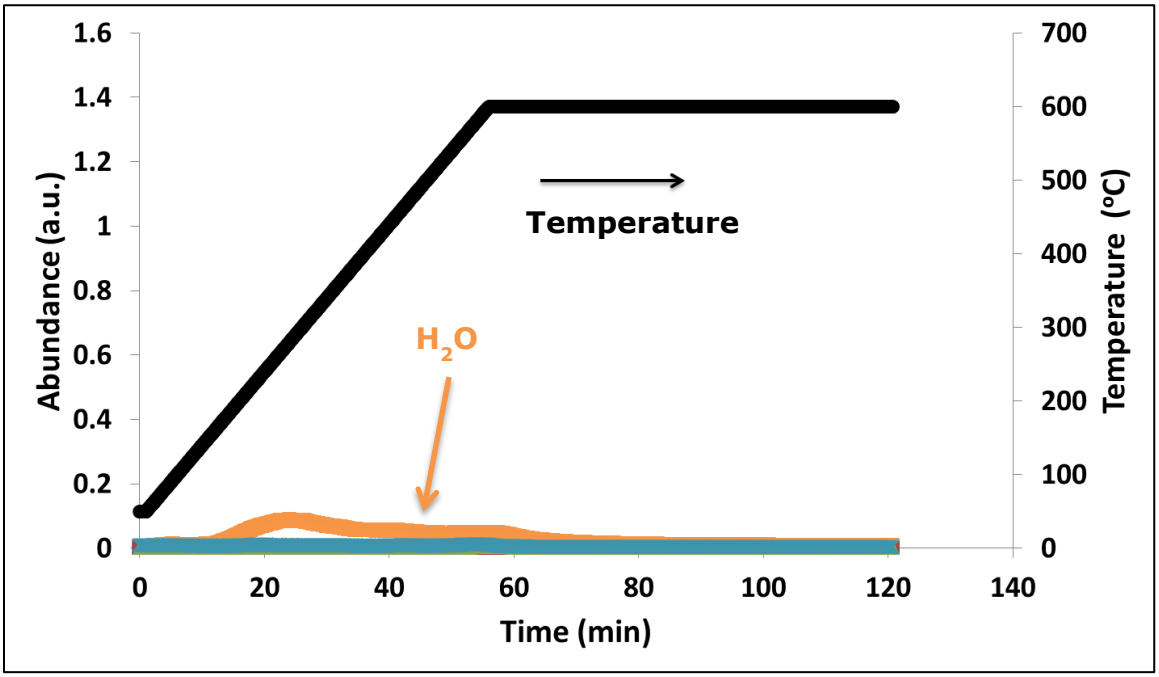

Figure 21. 3.4 nm 2% Pt Particles Washed Inert Experiment

This experiment involves heating the silica – immobilized washed platinum nanoparticles sized 3.4 nm and performed an inert, helium only, temperature – programmed experiment. When an inert gas, helium, is flown over a catalyst a reaction will not occur, as seen in Figure 21. The little amount of water seen in this experiment is desorption of water from the silica support.

3.3.2 Temperature – Programmed Reduction (TPR)

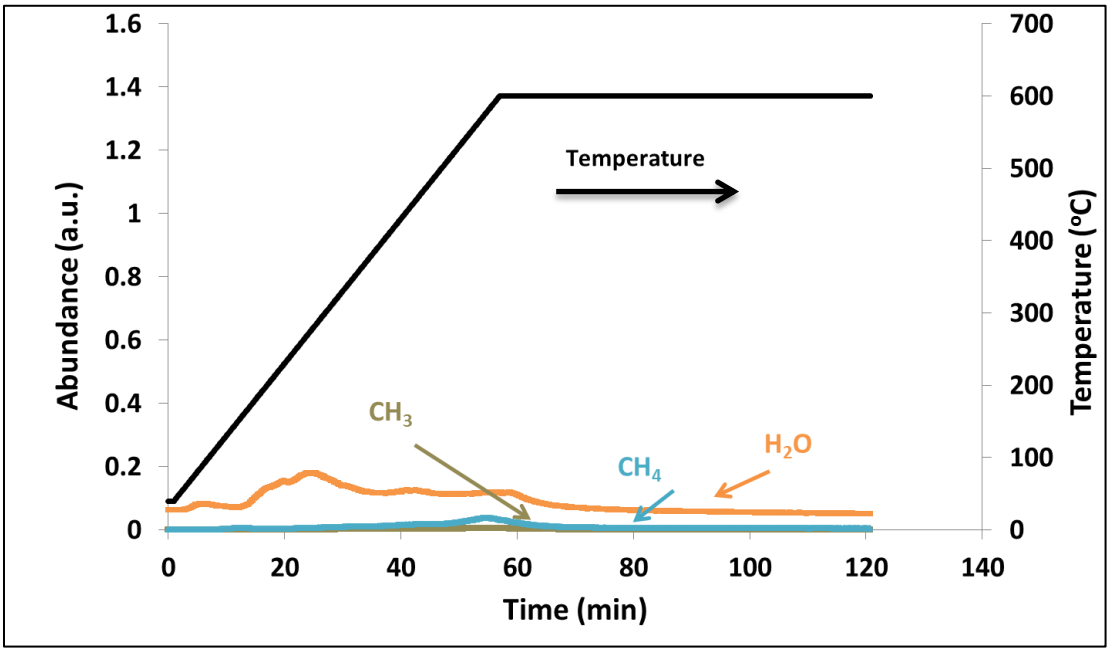

Figure 22. 3.4 nm Particles Washed TPR

The second experiment performed was temperature – programmed oxidation, 10% hydrogen in helium. During this experiment, it is expected that PVP and hydrogen will react to form water, methane, and other similar

methane fragments, CH_3. The small amount of water and methane formed proves that the particles were effectively washed. The abundance for all three molecules is under 0.2 a.u.

An experiment was performed by Borodko, et al. that studied the PVP decomposition of PVP on Pt particles in an H_2/argon environment. It was seen that the decomposition occurred above 200°C (Borodko, Lee and Joo). As seen in Figure 22 above, the decomposition also occurs after 200°C. Therefore, the results seen above are comparable to results seen previously in the literature.

3.3.3 Temperature – Programmed Oxidation (TPO): Washed – 3.4 nm And Unwashed Particles – 3.3 nm

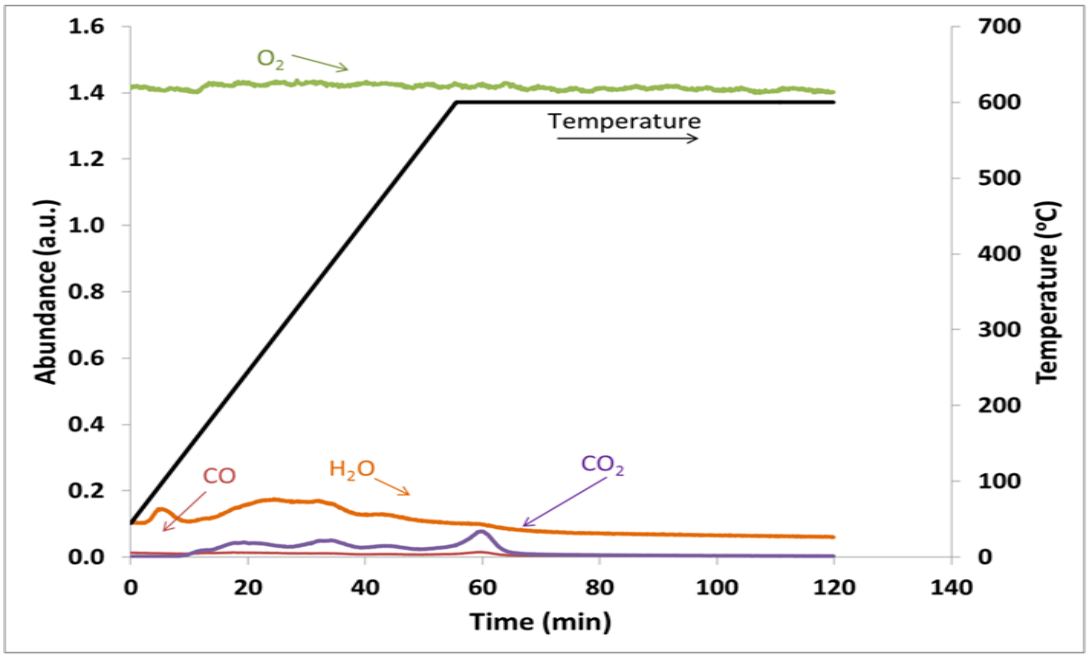

Figure 23. Washed 3.4 nm Particles TPO. Ramped At 10°C/min To 600°C And Held For One Hour

Temperature – programmed oxidation was performed for washed and unwashed particles. When PVP and oxygen are reacted together, carbon dioxide, carbon monoxide, and water are formed. The amount of PVP remaining on the particles is indicated by how much carbon dioxide, carbon monoxide, and water is formed. In Figure 23, only a small amount of carbon dioxide, carbon monoxide, and water is formed, under 0.2 a.u. for all three molecules.

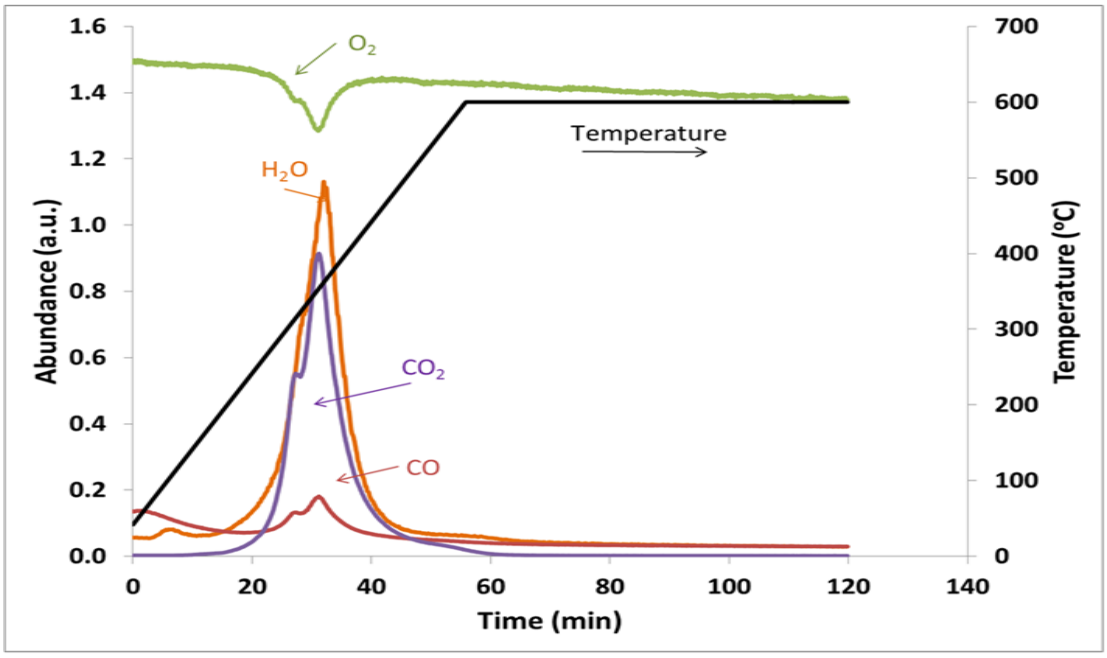

Figure 24. Unwashed 3.3 nm Particles TPO. Ramped At 10°C/min To 600°C And Held For One Hour

Figure 24, on the other hand, shows the same experiment using unwashed Pt particles. The amount of carbon dioxide, carbon monoxide, and water formed during this experiment is six times larger than the TPO experiment on the washed 3.4 nm particles immobilized on silica. This

difference proves that there is a much larger amount of PVP present on the unwashed particles and that the washed particles are effectively washed using the procedure seen in Chapter 2.

Another study was performed by Borodko, et al., to look at the decomposition of PVP in an oxygen atmosphere and Borodko's experiment showed that PVP decomposition occurs above 100^{o}C (Borodko, Lee and Joo). This is comparable to the study seen in Figure 24, the decomposition started around 100^{o}C.

3.4 Non – Sulfur Ethylene Hydrogenation Results

3.4.1 Experimental Graphs

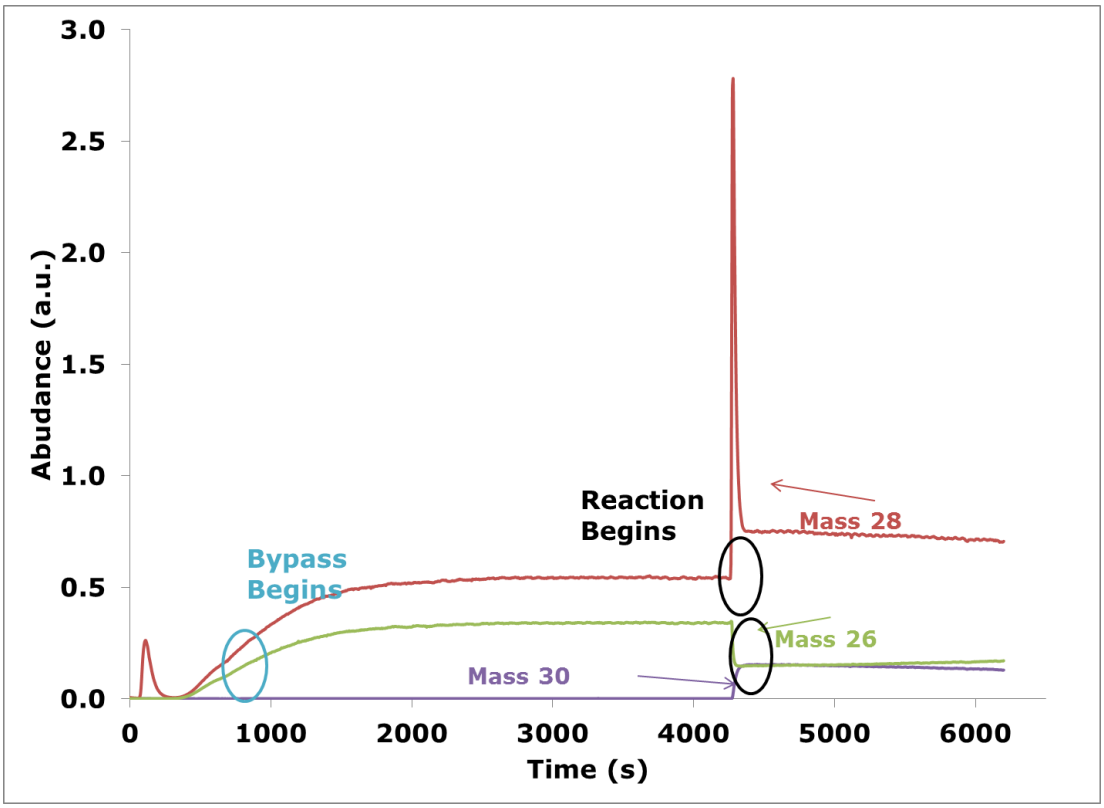

Figure 25. 2.0 nm Non – Sulfur Results: Ethylene Hydrogenation. (Bypass Performed At RT And Reaction Performed At 40°C)

For each non – sulfur experiment a bypass of the catalyst and a reaction over the catalyst was performed. The non – sulfur experiments were performed to ensure the particles were poisoned in the sulfur experiments. Both mass – to – charge of 26 and 28 are combinations of ethane and ethylene fragments and mass – to – charge of 30 indicates only the ethane molecule. Before the reaction begins, mass – to – charge of 30 has an abundance near zero and at steady state mass – to – charge of 28 has an

abundance of 0.5 and mass 26 has an abundance of 0.3. The absence of mass – to – charge of 30 confirms that there is no reaction occurring during the bypass.

During the reaction mass – to – charge 30 and mass – to – charge 28 and mass – to – charge 26 decreases until steady – state is reached. The formation of mass – to – charge 30 confirms that a reaction occurs when the gases are flown over the catalyst. The decrease of mass – to – charge 26 shows that mass – to – charge 26 is composed of more ethylene than ethane. The increase of mass – to – charge 28 on the other hand shows that mass – to – charge 28 is mainly composed of ethane. At steady state, mass – to – charge 30 had an abundance of 0.3 a.u., mass – to – charge 26 had an abundance of 0.35 a.u., and mass – to – charge 28 had an abundance of 0.75 a.u. The other non – sulfur experiments, seen in figures 26, 27, and 28, behaved similarly to the experiment described above.

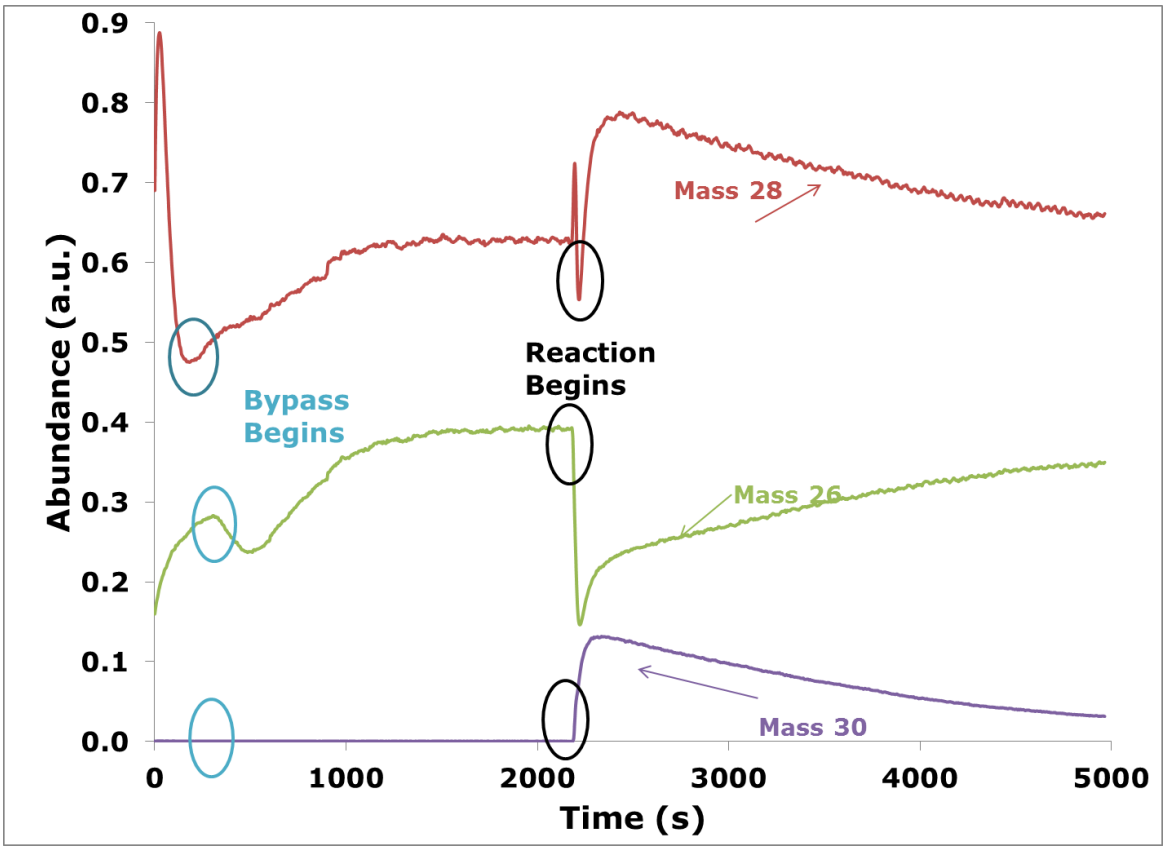

Figure 26. 3.4 nm Non - Sulfur Results: Ethylene Hydrogenation. (Bypass Performed At RT And Reaction Performed At 40°C)

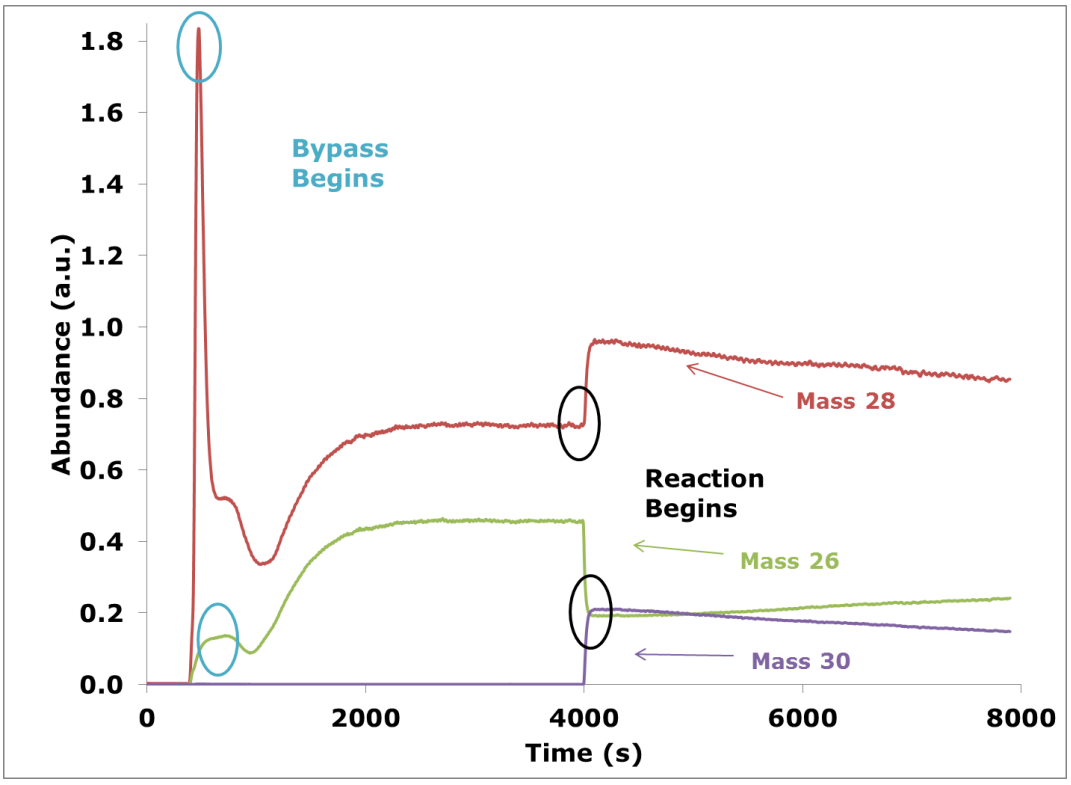

Figure 27. 4.3 nm Non - Sulfur Results: Ethylene Hydrogenation. (Bypass Performed At RT And Reaction Performed At 40°C)

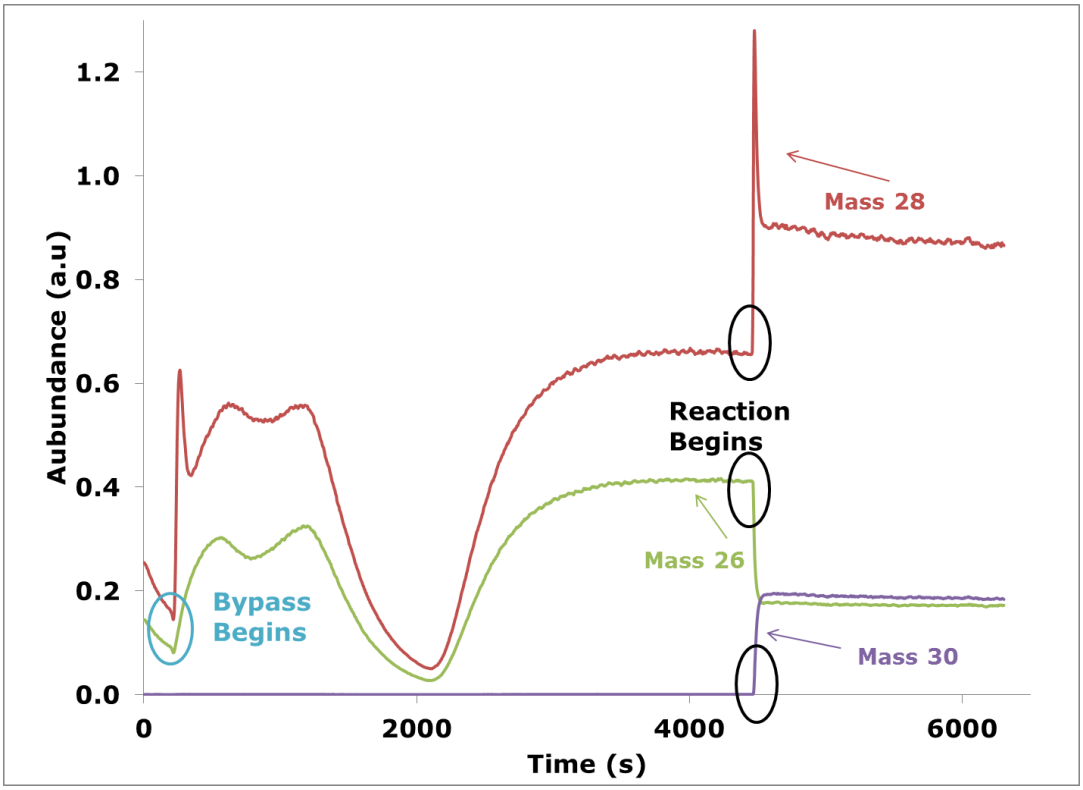

Figure 28. 6.8 nm Non - Sulfur Results: Ethylene Hydrogenation. (Bypass Performed At RT And Reaction Performed At 40°C)

3.4.2 Experimental Tables

Table 7. Ethylene Hydrogenation Conversion (40°C): No Sulfur

Size of Nanoparticle (nm)	Conversion (%)
2.0	75.6
3.4	42.3
4.3	69.9
6.8	79.1

The gases are fractionated in for the non – sulfur experiments as explained above. This makes finding the conversion a little more difficult. Equation 4 was used for both non – sulfur TOF calculations and sulfur TOF calculations.

$$TOF \ \ s^{-1} \ = \frac{molecules\ of\ ethylene\ converted}{avaliable\ Pt\ sites \ \ molecules}$$

Equation 4

Table 8. Ethylene Hydrogenation TOFs (40°C): No Sulfur

Size of Particle (nm)	TOF (s^{-1})
2.0	13.94
3.4	10.26
4.3	11.22
6.8	13.81

A study performed by Kuhn, et al. used Pt nanoparticles showed similar results to the values seen in Table 8. In the literature, for the size range of 2.0 – 5.0 nm, the values seen for TOF(s^{-1}) range from 11.4 – 15.3. As seen in Table 8, the values for TOF (s^{-1}) from the same range of sizes fall in the range seen in the literature, 11.22 – 13.94. The very similar results show that the experimental values and literature values agree with one another. In both cases, the TOF values compared to size can be considered

fairly constant. These results are comparable because and ethylene hydrogenation reaction was also performed in the literature and the synthesis conditions for sizes 2.0, 3.4, and 4.3 were similar to the process seen in the literature (Kuhn, Huang and Chia - Kuang).

The 6.8 nm particles synthesis was not taken from the literature and instead was synthesized by assuming that adding another seeded growth on the 4.3 nm, similar to the process of seeded growth for the 3.4 to 4.3 nm particles, would produce larger particles. For this reason, there is no literature value to compare ethylene hydrogenation of the 6.8 nm particle to the experimental value seen above. Although, since the values for the 2.0 – 4.3 nm TOF(s-1) are very similar it can be assumed that the TOF (s-1) value for 6.8 nm size should be similar to the smaller three sizes. It can be seen in Table 8, that the TOF value for the 6.8 nm size falls in the range for the smaller sizes, this proves that the TOF is similar to the other smaller sizes seen. It can be concluded that the TOF value for ethylene hydrogenation without sulfur for sizes 2.0 – 6.8 nm is fairly constant when compared with size.

3.5 Sulfur Ethylene Hydrogenation Results

3.5.1 Sulfur Concentration Used Calculation

To calculate the total ppm of sulfur used during the experiment the vapor pressure of thiophene must be calculated. Using the equation seen in Perry's Chemical Engineering Handbook, 6th edition, the vapor pressure of thiophene can be calculated at the chemical's temperature, 297.15 K.

$$Vapor\ Pressure = e^{93.193-\frac{7001.5}{T}-10.738\ln T+8.2308E-6*T^2}$$

Equation 5

At 297.15 K the vapor pressure of thiophene is 10.52 kPa. To calculate the ppm of sulfur used in the experiment multiply the vapor pressure of thiophene by the thiophene flow fraction (1/201) and 1E6. At room temperature this resulted in a sulfur concentration of 492.25 ppm.

3.5.2 Results Of Gas Chromatography Experiments

Table 9. Averaged Steady State Bypass Results For Sulfur Experiments

Size of Particle (nm)	Area of C_2H_4 (a.u.)	Area of C_2H_6 (a.u.)
2.0	33920	0
3.4	32680	0
4.3	32879	0
6.8	32828	0

Table 10. Average Steady State Reaction Results For Sulfur Experiments

Size of Particle (nm)	Area of C_2H_4 (a.u.)	Area of C_2H_6 (a.u.)
2.0	32384	624
3.4	32728	467
4.3	32515	467
6.8	32612	435

Tables 9 and 10 show the averages for the steady state values of the areas under the curve for both ethane and ethylene during the gas chromatography sulfur experiments. During the bypass experiments, there was no signal for ethane seen. This indicates that signals during the ethylene hydrogenation gas chromatography experiments there is no conversion during the bypass portion. This also indicates that the gases during the reaction portion of the experiment are not fractionated and the entire ethylene signal is only ethylene and the entire ethane signal is only ethane. The gases for the gas chromatograph are not fractionated resulting in easier calculations for the conversion.

Table 11. Conversion Values For Sulfur Experiments

Size of Particle (nm)	Conversion (%)
2.0	2.3
3.4	1.4
4.3	1.3
6.8	1.3

$$\boldsymbol{Conversion}\ \ \% \ = \frac{(\boldsymbol{Area\ of Ethane})}{\boldsymbol{Area\ of\ Ethane + Area\ of\ Ethylene}}$$

Equation 6

Table 12. TOF For Sulfur Experiments

Size of Nanoparticle (nm)	TOF (s^{-1})
2.0	0.008
3.4	0.021
4.3	0.032
6.8	0.037

A study performed by Rioux, et al. performs an ethylene hydrogenation reaction with and without carbon monoxide poisoning. The sizes of the Pt particles in this study range from 1.7 – 7.1 nm. When the catalyst is poisoned the turnover frequency decreased when the particles were poisoned (Rioux, Komor and Song). Similar to the literature, when the Pt particles were poisoned, in this case with sulfur, the turnover frequency decreased as compared to when the particles were not poisoned when performing an ethylene hydrogenation reaction.

3.6 Sulfur Tolerance Of Platinum Nanoparticles

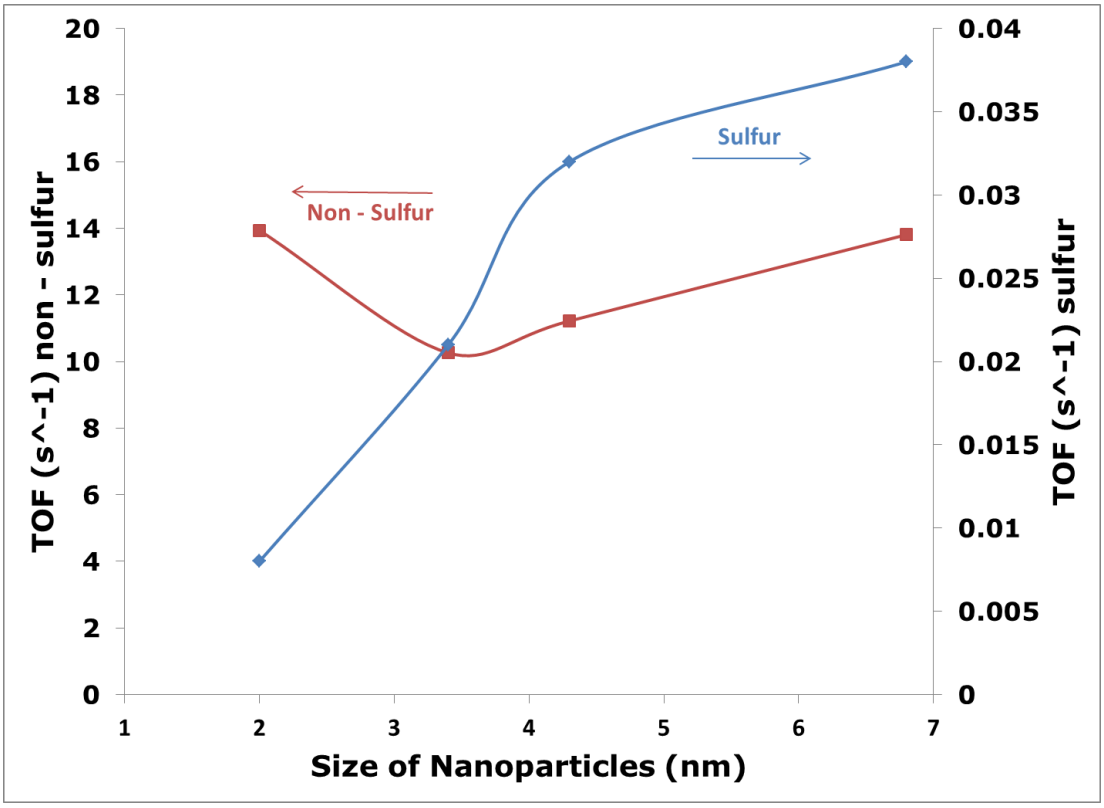

Figure 29. Comparison Of Sulfur Vs. Non - Sulfur Results

Figure 29 shows the final results of the ethylene hydrogenation reactions with and without sulfur. The TOF of the non – sulfur experiments range from 10 – 14 s^{-1}. Since all the TOFs are in the same magnitude, it can be said that these results are fairly constant as a function of catalyst size. Similar results were seen in a study by Kuhn et al. also showed that during an ethylene hydrogenation reaction without any poisoning present that the TOF is constant with changing size of Pt nanoparticles.

The sulfur experiment portion of the graph shows a different story. The magnitudes of the TOF for sizes 3.4 – 6.8 nm are all the same. It could be said that the TOF is fairly constant with increasing size and there is an additional reason that the 2 nm experiment is one magnitude smaller than the others. On the other hand, it is seen that for all four sizes that when the Pt nanoparticles are poisoned with sulfur the TOF increases with increasing size. This leaves two possible explanations for how the size affects a Pt nanoparticle when it is poisoned with sulfur. One of the explanations is that the sulfur tolerance of platinum nanoparticles is not affected by changing nanoparticle size. The other explanation is that the sulfur tolerance increases with increasing size of Pt nanoparticles.

The sulfur tolerance being unaffected by the size of the nanoparticles could be explained by the different synthesis technique and washing technique used on the 2 nm Pt particles. The PVP of the 2 nm particle size could have not been effectively washed. This could cause the Pt particles to have less activity when poisoned due to the PVP blocking some of the active sites where the reaction could occur. By this logic, it would be expected that the non – sulfur experiment would also have less activity, which was not the case. The 2 nm non – sulfur experiment had a TOF of 13.94 s^{-1}, which was the highest seen for all sizes during the non – sulfur experiments.

To test the theory of the PVP not being effectively washed off the 2 nm particles, two TPO experiments were performed one on unwashed 2 nm Pt particle and one on washed 2 nm Pt particle. Figure 30 and 31 show the

results of both the washed and unwashed TPO experiments. Figure 30 shows that there was oxidation of PVP that started to occur at 400^{o}C. Normally, as mentioned above, PVP decomposes above 100^{o}C and here PVP is seen to decompose at 400^{o}C, which is consistent with the literature (Borodko, Lee and Joo). Figure 31 on the other hand shows the opposite effect. Figure 31 does not show any abundance of CO_2, CO, and H_2O, until in the 600^{o}C range where there is a small amount of H_2O. This is higher than what is seen in the 3.4 nm particles and this could be due to the difference in size of the particles. This small amount of water is due to water that absorbed onto the catalyst from the atmosphere. From analysis of Figure 30 and 31, it is concluded that the particles were effectively washed. Therefore, the TOF of the 1.5 nm particles was not lower because the particles were not effectively washed. This means that sulfur tolerance of Pt nanoparticles is not fairly constant with size and that there is some size effect present.

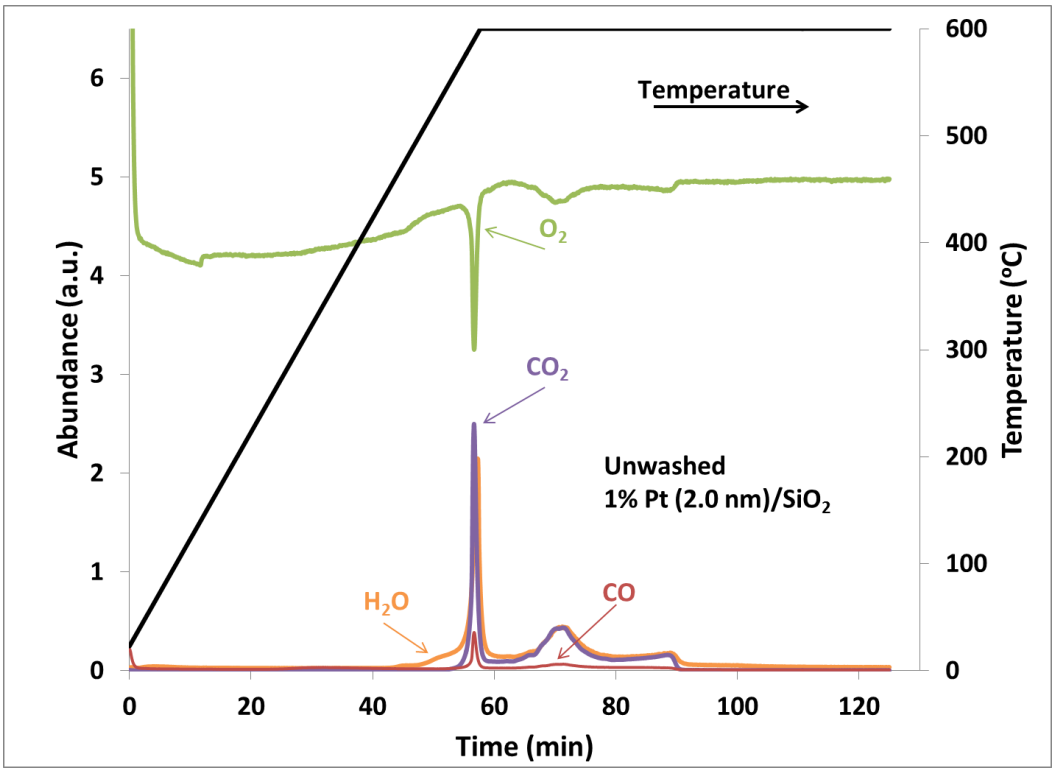

Figure 30. Unwashed TPO 1.5 nm Experiment. (Held At 600°C For One Hour, Ramped At 10°C/min From RT)

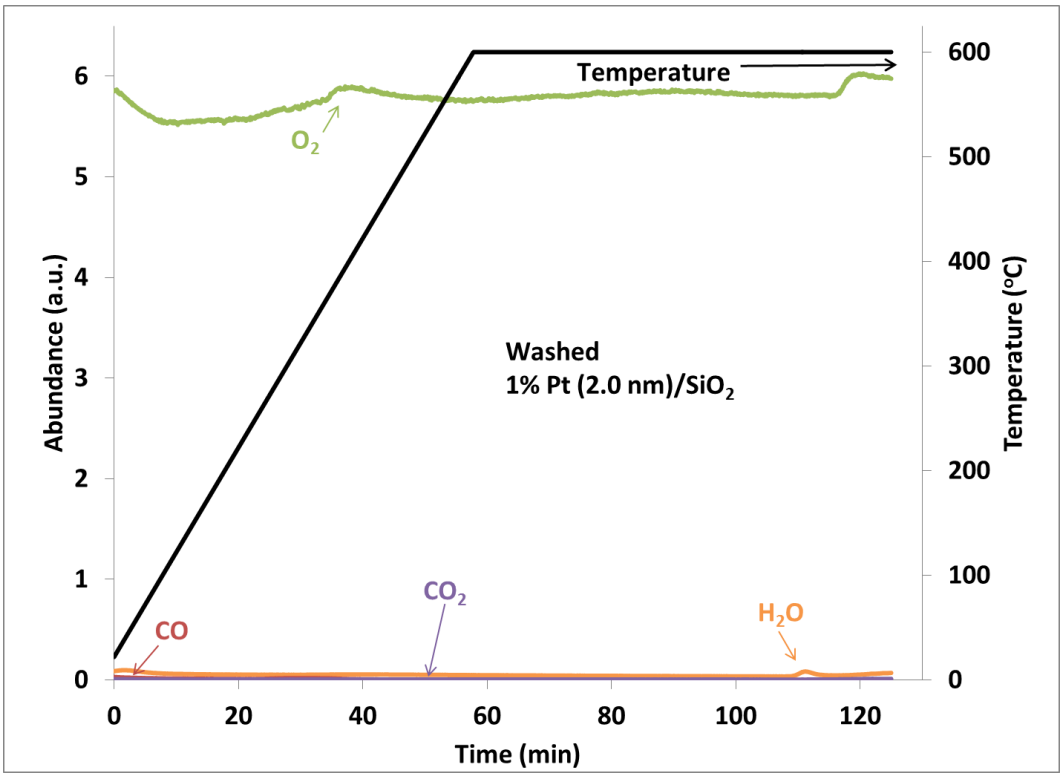

Figure 31. Washed TPO 1.5 nm Experiment. (Held At 600°C For One Hour, Ramped At 10°C/min)

This leaves the explanation that sulfur binds more strongly to the smaller particles (Wang and Iglesia). A face – centered – cubic (FCC) molecule, such as (111) Pt, has a coordination number of 12 for its center molecule. There are 6 molecules directly surrounding the center molecule, three molecules in contact on the top of the center molecule, and three molecules in contact on the bottom of the molecule. A surface molecule has a coordination of 9, since it will not have the top three molecules. Coordination number is the number of nearest neighbors a molecule will have (i.e. the

number of bonds a molecule could make). Below in Table 13 give roughly the coordination number of each size of Pt nanoparticles synthesized (Che and Bennett).

Table 13. Coordination Numbers (Che and Bennett)

Size of Pt Particle (nm)	Coordination Number
2.0	4.5
3.4	7.7
4.3	8.1
6.8	8.6

As seen in Table 13, as the particle size increases the coordination number will increase and eventually steady out. If the coordination number is larger in an FCC material (where total possible coordination number is 12 as mentioned above), there will be spots for a reaction intermediate to bond. Other the other hand, smaller particles will have less neighboring molecules, leaving more spaces for additional molecules to bond to the Pt molecule. The smallest Pt molecule has a coordination number of 4.5 this means that sulfur has the opportunity to bond more strongly to the molecule because there are more bonds available. If the sulfur binds more strongly, this will cause less activity as seen in an experiment done by Wang et al. and the experiments performed above (Wang and Iglesia). As the size of the particle increases, the coordination number will steady out resulting in less change in the

coordination number, as seen in Table 13 (Che and Bennett). This will cause a smaller increase in the activity as a function of particle size as the coordination number reaches steady state. This in turn, shows that the larger Pt particles are more sulfur tolerant.

In addition, Figure 32, shows the difference in the rate between the sulfur and non – sulfur experiments. It is expected that, as seen, the rate of the particles will decrease as size increases. This is due to the dispersion, which also decreases as particle size increases. Dispersion is the number of surface atoms over the number of total atoms in the particle. As dispersion increases, the amount of atoms exposed increases which will increase the rate. The rate is increased because "intrinsic catalytic activity, as a general rule, proportional to the concentration of active sites available for catalysis". This means when a catalyst is not affected by poisoning, coking, etc., the activity of the catalyst should decrease with increasing size (Bartholomew).

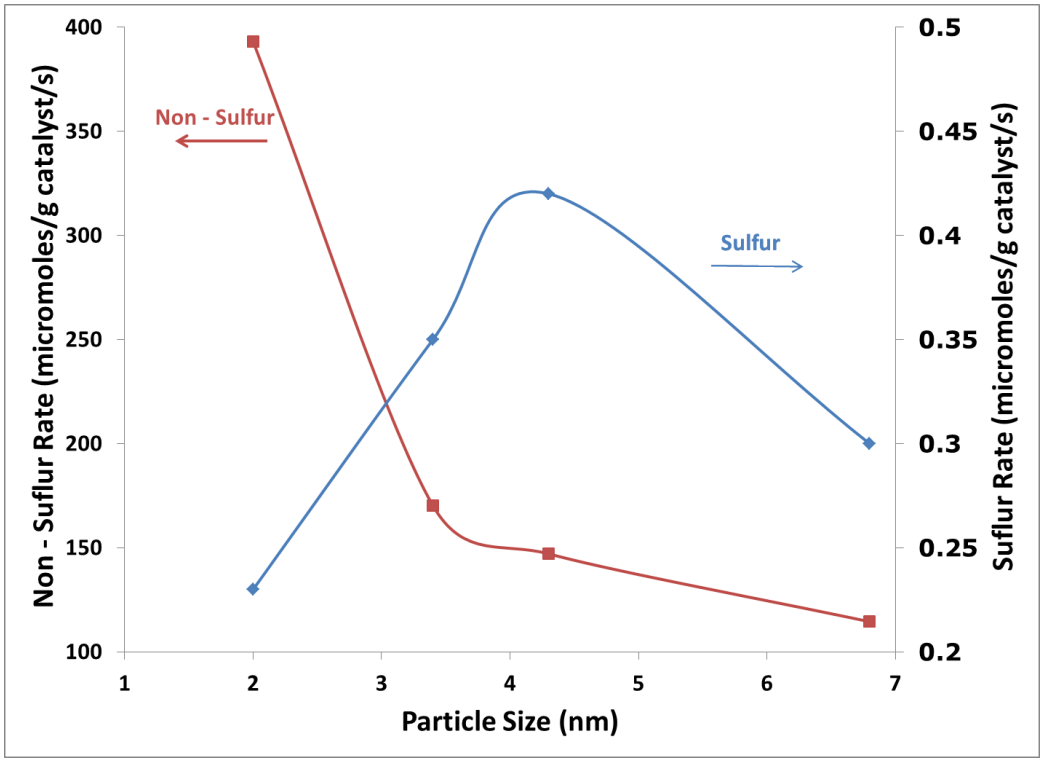

Figure 32. Non - Sulfur And Sulfur Rate Vs. Particle Size

In the case of the rate for the sulfur experiments, a maximum is seen at the 4.3 nm particles and a minimum at the 2 nm particle size. Since the rate is the highest for the non – sulfur experiment and the smallest when poisoned, it can be said that during hydrogenation when poisoned by sulfur the smallest particle is not the best to use. The rate of the 2 nm Pt particles is affected more by being poisoned than any of the other sizes tested.

Chapter 4: Conclusions

In conclusion, this project has shown that sulfur tolerance does change as a function of particle size. The larger particles are more sulfur tolerant than the smaller particles. Although the 6.8 nm particle has the best TOF, in application of using a catalyst in industry, the rate of the catalyst is usually of the most concern. If the current results were to be applied to a more cost effective bi – metallic catalyst, the 4.3 nm Pt particles would be a good size to start experimenting. As the size of the particle increased, the activity of the particle increased due the sulfur bonding more strongly to the smaller particles. This will cause less activity. Resolution of this issue can move the project into other areas. These areas include, bi – metallic catalyst synthesis, testing of the catalyst in an actual fuel stream with low sulfur concentration to test removal capabilities, or testing the best size (4.3 nm) with various supports to make sure silica is the best to use.

References

Annenberg Learner. Unit 8: Water Resources//Section 6: Depletion of Freshwater Resources. 2011. 28 October 2011 <xhttp://learner.org/courses/envsci/unit/text.php?unit=8&secNum=6>.

Bartholomew, C.H. and Farrauto, R.J. Fundamentals of Industrial Catalytic Processes. Hoboken, New Jersey: John Wiley & Sons, Inc., 2006.

Bihan, Lionel Le and Yuji Yoshimura. "Control of hydrodesulfurization and hydrodearomatization properties over bimetallic Pd-Pt catalysts supported on Yb-modified USY zeolite." Fuel (2002): 491-494.

Borodko, Yuri, et al. "Probing the Interaction of Poly(vinylpyrrolidone) with Platinum Nanocrystals by UV - Rama and FTIR." Journal of Physical Chemistry B (2006): 23052 - 23059.

—. "Spectroscopic Study of the Thermal Degradation of PVP - Capped Rh and Pt Nanoparticles in H2 and O2 Environments." Journal of Physical Chemistry C (2010): 1117 - 1126.

Brandon, David and Wayne D. Kaplan. Microstructural Characterization of Materials. West Sussex, England: John Wiley & Sons Ltd., 2008.

British Zeolite Association. What are Zeolites? May 2001. 25 September 2011 <http://www.bza.org/zeolites.html>.

Brunet, Slyvette, et al. "On the hydrodesulfization of FCC gasoline: a review." Applied Catalysis (2005): 143 - 172.

Cattenot, Martine, et al. "Mechanism of carbon - nitrogen bond scission in the presence of H2S on Pt supported catalysts." Catalysis Letters (2005): 171 - 176.

Che, Michael and Carroll O. Bennett. "The Influence of Particle Size on the Catalytic Properties of Supported Metals." Advances in Catalysis (1989): 55 - 172.

Cheah, Singfoog, Daniel L. Carpenter and Kimberly A. Magrini - Bair. "Review of Mid - to - High Temperature Sulfur Sorbents for Desulfization of Biomass - and Coal - derived Syngas." Energy & Fuels (2009): 5291 - 5307.

Environment News Service. "U.S. Air Quality Agencies Urge Lower Sulfur in Gas." 2011 2 November. Environment News Service. 20 January 2012 <http://www.ens-newswire.com/ens/nov2011/2011-11-02-093.html>.

Environmental Protection Agency. "Air Pollution." Emission. 2009.

—. Effects of Acid Rain. 8 June 2007. 4 March 2011 <http://www.epa.gov/acidrain/effects/>.

—. Effects of Acid Rain - Human Health. 13 May 2009. 4 March 2011 <http://www.epa.gov/acidrain/effects/health.html>.

—. "Haze How Air Pollution Affects the View." 1999. Environmental Protection Agency. 4 March 2011 <http://www.epa.gov/ttncaaa1/t1/fr_notices/haze.pdf>.

—. Sulfur Dioxide Emissions. 17 Feburary 2010. 1 March 2011 <http://cfpub.epa.gov/eroe/index.cfm?fuseaction=detail.viewInd&lv=list.listByAlpha&r=219694&subtop=341>.

—. Sulfur Dioxide Emissions: Charts and Graphs. 17 Feburary 2010. 1 March 2011 <http://cfpub.epa.gov/eroe/index.cfm?fuseaction=detail.viewMidImg&ch=46&lShowInd=0&subtop=341&lv=list.listByChapter&r=219694>

Fujikawa, Takashi, et al. "Aromatic hydrogenation of distillates over SiO2 - Ali2O3 - supported noble metal catalysts." Applied Catalysis (2000): 253 - 261

Guo, Hongli, Yingyong Sun and Roel Prins. "Hydrodesulfurization of 4,6 - dimethyldibenzotiophene over Pt supported on gamma - Al2O3, SBA - 15, and HZSM - 5." Catalysis Today (2007): 249 - 253.

Harvi Velasquez, Hervin Rameriz, Jose Diaz, Marlene Gonzalez de Nava, Beatrice Sosa de Borrego, Joes Morales. "Determination of atmospheric sulfur dioxide by ion chromatography in the city of Cabimas, Venezuela." Journal of Chromatography A (1996): 295 - 299.

Kabe, Toshiaki, et al. "Hydrodesulfurization and Hydrogenation Reactions on Noble Metal Catalysts." Journal of Catalysis (2000): 191 - 198.

Knudsen, Kim G., Barry H. Cooper and Henrik Topsoe. "Catalyst and process technologies for ultra low sulfur diesel." Applied Catalysis (1999): 205 - 215.

Kuhn, John N., et al. "Structure Sensitivity of Carbon - Nitrogen Ring Opening: Impact of Platinum Particle Size from below 1 to 5 nm upon Pyrrole Hydrogenation Product Selectivity over Monodisperse Platinum Nanoparticles Loaded onto Mesoporous Silica." J. Am. Chem. Soc. (2008): 14026 - 14027.

Kuo, Yeong - Jen and Bruce J. Tatarchuk. "Hydrogenation and Hydrodesulfurization over Sulfided Ruthenium Catalysts." Journal of Catalysis (1988): 229 - 249.

L.G. Wade, Jr. Organic Chemistry Sixth Edition. Upper Saddle River: Pearson Prentice Hall, 2006.

Lewandowski, M., et al. "Catalytic performance of platinum doped tungsten carbide in simultaneous hydrogenation and hydrodesulphurization." Applied Catalysis B: Environmental (2010): 241 - 249.

Matsui, Takashi, et al. "Effect of coexistence of nitrogen compounds on the sulfur tolerance and catalytic activity of Pd and Pt monometallic catalysts supported on high - silica USY zeolite and amorphous silica." Applied Catalysis A: General (2005): 137-144.

—. "Effect of noble metal particle size on the sulfur tolerance of monometallic Pd and Pt catalysts supported on high silicia USY zeolite." Applied Catalysis (2005): 249-257.

Merino, Lourdes I., Aristobulo Centeno and Sonia A. Giraldo. "Influence of the activation conditions of bimetallic catalysts NM - Mo/gamma-Al2O3 (NM = Pt, Pd and Ru) on the activity in HDT reactions." Applied Catalysis (2000): 61-68.

Michaelides, A. and P. Hu. "Hydrogenation of S to H2S on Pt(111): A first - principles study." Journal of Chemical Physics (2001): 8570 - 8574.

Miller, J. T. and D. C. Koningsberger. "The Origin of Sulfur Tolerance in Supported Platinum Catalysts: The Relationship between Structural and Catalytic Properties in Acidic and Alkaline Pt/LTL." Journal of Catalysis (1996): 209 - 219.

Niquille - Rothlisberger, Adeline and Roel Prins. "Hydrodesulfurization of 4,6 - dimethyldibenzothiophene over Pt, Pd, and Pt - Pd catalysts supported on amphorous silica - alumina." Catalysis Today (2007): 198 - 207.

Perry, Robert H. and Don Green. Perry's Chemical Engineering Handbook. New York: McGraw-Hill Book Company, 1984.

Pessayre, Stephanie, et al. "Platinum Doped Hydrotreating Catalysts for Deep Hydrodesulfization of Diesel Fuels." Ind. Eng. Chem. Res. (2007): 3877 - 3883.

Qian, Weihua, et al. "Hydrodesulfuization of dibenzothiophene and hydrogenation of phenanthrene on alumina-supported Pt and Pd catalysts." Appled Catalysis (1999): 81-88.

Reinhoudt, H.R., et al. "Testing and characterisation of Pt/ASA for deep HDS reactions." Fuel Processing Technology (1999): 117-131.

Rioux, R. M., et al. "High - Surface - Area Catalyst Design: Synthesis, Characterization, and Reaction Studies of Platinum Nanoparticles in Mesoporous SBA - 15 Silica." J. Phys. Chem. B (2005): 2192 - 2202.

Rioux, Robert M., et al. "Kinetics and mechanism of ethylene hydrogenation posioned on CO on silica - supported monodisperse Pt nanoparticles." Journal of Catalysis (2008): 1 - 11.

Robinson, W.R.A.M, et al. "Development of deep hydrodesulfurization catalysts II. NiW, Pt and Pd catalysts tested with (substituted) dibenzothiophene." Fuel Processing Technology (1999): 103 - 116.

Rothlisberger, Adeline and Prins, Roel. "Intermediates in the hydrodesulfurization of 4,6 - dimethyl - dibenzothiophene over Pd/y - Al2O3." Journal of Catalysis (2005): 229 - 240.

Shackelford, James F. Materials Science for Engineers. Upper Saddle River, NJ: Prentice-Hall, Inc., 2000.

Shell. Shell Diesel. n.d. 4 March 2011 <http://www.shell.us/home/content/usa/products_services/on_the_road/fuels/diesel/>.

Sufiyanov, R. Sh., A. V. Katalymov and G. Yu Gol'berg. "Environmental Implications of More Efficient Fuel Processing." Environmental Protection (2009): 73 - 76.

Sun, Yinyong and Prins, Roel. "Hydrodesulfization of 4,6 - dimethyldibenzothiophene over Noble Metal Supported on Mesoporous Zeolites." Heterogenous Catalysis (2008): 8478 - 8481.

Teranishi, T., et al. "Size Control of Monodispersed Pt Nanoparticles and Their 2D Organization by Electrophretic Deposition." J. Phys. Chem. B (1999): 3818 - 3827.

U.S. Environmental Protection Agency Office of Transportation and Air Quality. "Greenhouse Gas Emissions from the U.S. Transportation Sector, 1990 - 2003." 2006. Environmental Protection Agency. 6 May 2011 <http://www.epa.gov/otaq/climate/420r06003.pdf>.

Vit, Zdenek, Josef Cinibulk and Daniela Gulkova. "Promotion of Mo/Al2O3 sulfide catalyst by noble metals in simulataneous hydrodesulfization of thiophene and hydrodenitrogenation of pyridine: a comparitve study." Applied Catalysis (2004): 99-107.

Wang, Huamin and Enrique Iglesia. "Thiophene hydrodesulfurization catalysis on supported Ru clusters: Mechanism and site requirements for hydrogenation and desulfurization pathways." Journal of Catalysis (2010): 245-256.

Zhanghuai, Suo, et al. "Influence of Au promoter on hydrodesulfurization activity of thiophene over sulfided Au-Ni/SiO2 bimetallic catalysts." Catalysis Communications (2009): 1174-1177.

Appendices

Appendix A: Journal Permissions

AMERICAN INSTITUTE OF PHYSICS LICENSE TERMS AND CONDITIONS

Mar 28, 2012

Click here for Payment Terms and Conditions.

All payments must be made in full to CCC. For payment instructions, please see information listed at the bottom of this form.

License Number	2779630888770
Order Date	Oct 31, 2011
Publisher	American Institute of Physics
Publication	Journal of Chemical Physics
Article Title	Hydrogenation of S to H2S on Pt(111): A first-principles study
Author	A. Michaelides, P. Hu
Online Publication Date	Dec 31, 1969
Volume number	115
Issue number	18
Type of Use	Thesis/Dissertation
Requestor type	Student
Format	Electronic
Portion	Figure/Table
Number of figures/tables	1
Title of your thesis / dissertation	Effect of Particle Size on Sulfur Deactivation of Platinum Nano - Catalysts
Expected completion date	May 2012
Estimated size (number of pages)	100
Total	0.00 USD

Terms and Conditions

American Institute of Physics -- Terms and Conditions: Permissions Uses

American Institute of Physics ("AIP") hereby grants to you the non-exclusive right and license to use and/or distribute the Material according to the use specified in your order, on a one-time basis, for the specified term, with a maximum distribution equal to the number that you have ordered. Any links or other content accompanying the Material are not the subject of this license.

Appendix A Continued

1. You agree to include the following copyright and permission notice with the reproduction of the Material: "Reprinted with permission from [FULL CITATION]. Copyright [PUBLICATION YEAR], American Institute of Physics." For an article, the copyright and permission notice must be printed on the first page of the article or book chapter. For photographs, covers, or tables, the copyright and permission notice may appear with the Material, in a footnote, or in the reference list.
2. If you have licensed reuse of a figure, photograph, cover, or table, it is your responsibility to ensure that the material is original to AIP and does not contain the copyright of another entity, and that the copyright notice of the figure, photograph, cover, or table does not indicate that it was reprinted by AIP, with permission, from another source. Under no circumstances does AIP, purport or intend to grant permission to reuse material to which it does not hold copyright.
3. You may not alter or modify the Material in any manner. You may translate the Material into another language only if you have licensed translation rights. You may not use the Material for promotional purposes. AIP reserves all rights not specifically granted herein.
4. The foregoing license shall not take effect unless and until AIP or its agent, Copyright Clearance Center, receives the Payment in accordance with Copyright Clearance Center Billing and Payment Terms and Conditions, which are incorporated herein by reference.
5. AIP or the Copyright Clearance Center may, within two business days of granting this license, revoke the license for any reason whatsoever, with a full refund payable to you. Should you violate the terms of this license at any time, AIP, American Institute of Physics, or Copyright Clearance Center may revoke the license with no refund to you. Notice of such revocation will be made using the contact information provided by you. Failure to receive such notice will not nullify the revocation.
6. AIP makes no representations or warranties with respect to the Material. You agree to indemnify and hold harmless AIP, American Institute of Physics, and their officers, directors, employees or agents from and against any and all claims arising out of your use of the Material other than as specifically authorized herein.
7. The permission granted herein is personal to you and is not transferable or assignable without the prior written permission of AIP. This license may not be amended except in a writing signed by the party to be charged.
8. If purchase orders, acknowledgments or check endorsements are issued on any forms containing terms and conditions which are inconsistent with these provisions, such inconsistent terms and conditions shall be of no force and effect. This document, including the CCC Billing and Payment Terms and Conditions, shall be the entire agreement between the parties relating to the subject matter hereof.

Appendix A Continued

This Agreement shall be governed by and construed in accordance with the laws of the State of New York. Both parties hereby submit to the jurisdiction of the courts of New York County for purposes of resolving any disputes that may arise hereunder.

If you would like to pay for this license now, please remit this license along with your payment made payable to "COPYRIGHT CLEARANCE CENTER" otherwise you will be invoiced within 48 hours of the license date. Payment should be in the form of a check or money order referencing your account number and this invoice number RLNK500656009. Once you receive your invoice for this order, you may pay your invoice by credit card. Please follow instructions provided at that time.

Make Payment To:
Copyright Clearance Center
Dept 001
P.O. Box 843006
Boston, MA 02284-3006

For suggestions or comments regarding this order, contact RightsLink Customer Support: customercare@copyright.com or +1-877-622-5543 (toll free in the US) or +1-978-646-2777.

Gratis licenses (referencing $0 in the Total field) are free. Please retain this printable license for your reference. No payment is required.

Appendix A Continued

ELSEVIER LICENSE
TERMS AND CONDITIONS

Mar 28, 2012

This is a License Agreement between Lyndsey M Baldyga ("You") and Elsevier ("Elsevier") provided by Copyright Clearance Center ("CCC"). The license consists of your order details, the terms and conditions provided by Elsevier, and the payment terms and conditions.

All payments must be made in full to CCC. For payment instructions, please see information listed at the bottom of this form.

Supplier	Elsevier Limited The Boulevard,Langford Lane Kidlington,Oxford,OX5 1GB,UK
Registered Company Number	1982084
Customer name	Lyndsey M Baldyga
Customer address	15425 Plantation Oaks Dr. Tampa, FL 33647
License number	2779630248383
License date	Oct 31, 2011
Licensed content publisher	Elsevier
Licensed content publication	Applied Catalysis B: Environmental
Licensed content title	Catalytic performance of platinum doped tungsten carbide in simultaneous hydrodenitrogenation and hydrodesulphurization
Licensed content author	M. Lewandowski,P. Da Costa,D. Benichou,C. Sayag
Licensed content date	12 January 2010
Licensed content volume number	93

A**ppendix A Continued**

Licensed content issue number	3-4
Number of pages	9
Start Page	241
End Page	249
Type of Use	reuse in a thesis/dissertation
Portion	figures/tables/illustrations
Number of figures/tables/illustrations	1
Format	electronic
Are you the author of this Elsevier article?	No
Will you be translating?	No
Order reference number	
Title of your thesis/dissertation	Effect of Particle Size on Sulfur Deactivation of Platinum Nano - Catalysts
Expected completion date	May 2012
Estimated size (number of pages)	100
Elsevier VAT number	GB 494 6272 12
Permissions price	0.00 USD
VAT/Local Sales Tax	0.0 USD / 0.0 GBP
Total	0.00 USD
Terms and Conditions	

INTRODUCTION

1. The publisher for this copyrighted material is Elsevier. By clicking "accept" in connection with completing this licensing transaction, you agree that the following terms and conditions apply to this transaction (along with the Billing and Payment terms and conditions established by Copyright Clearance Center, Inc. ("CCC"), at the time that you opened your Rightslink account and that are available at any time at http://myaccount.copyright.com).

Appendix A Continued

GENERAL TERMS

2. Elsevier hereby grants you permission to reproduce the aforementioned material subject to the terms and conditions indicated.

3. Acknowledgement: If any part of the material to be used (for example, figures) has appeared in our publication with credit or acknowledgement to another source, permission must also be sought from that source. If such permission is not obtained then that material may not be included in your publication/copies. Suitable acknowledgement to the source must be made, either as a footnote or in a reference list at the end of your publication, as follows:

"Reprinted from Publication title, Vol /edition number, Author(s), Title of article / title of chapter, Pages No., Copyright (Year), with permission from Elsevier [OR APPLICABLE SOCIETY COPYRIGHT OWNER]." Also Lancet special credit - "Reprinted from The Lancet, Vol. number, Author(s), Title of article, Pages No., Copyright (Year), with permission from Elsevier."

4. Reproduction of this material is confined to the purpose and/or media for which permission is hereby given.

5. Altering/Modifying Material: Not Permitted. However figures and illustrations may be altered/adapted minimally to serve your work. Any other abbreviations, additions, deletions and/or any other alterations shall be made only with prior written authorization of Elsevier Ltd. (Please contact Elsevier at permissions@elsevier.com)

6. If the permission fee for the requested use of our material is waived in this instance, please be advised that your future requests for Elsevier materials may attract a fee.

7. Reservation of Rights: Publisher reserves all rights not specifically granted in the combination of (i) the license details provided by you and accepted in the course of this licensing transaction, (ii) these terms and conditions and (iii) CCC's Billing and Payment terms and conditions.

8. License Contingent Upon Payment: While you may exercise the rights licensed immediately upon issuance of the license at the end of the licensing process for the transaction, provided that you have disclosed complete and accurate details of your proposed use, no license is finally effective unless

Appendix A Continued

and until full payment is received from you (either by publisher or by CCC) as provided in CCC's Billing and Payment terms and conditions. If full payment is not received on a timely basis, then any license preliminarily granted shall be deemed automatically revoked and shall be void as if never granted. Further, in the event that you breach any of these terms and conditions or any of CCC's Billing and Payment terms and conditions, the license is automatically revoked and shall be void as if never granted. Use of materials as described in a revoked license, as well as any use of the materials beyond the scope of an unrevoked license, may constitute copyright infringement and publisher reserves the right to take any and all action to protect its copyright in the materials.

9. Warranties: Publisher makes no representations or warranties with respect to the licensed material.

10. Indemnity: You hereby indemnify and agree to hold harmless publisher and CCC, and their respective officers, directors, employees and agents, from and against any and all claims arising out of your use of the licensed material other than as specifically authorized pursuant to this license.

11. No Transfer of License: This license is personal to you and may not be sublicensed, assigned, or transferred by you to any other person without publisher's written permission.

12. No Amendment Except in Writing: This license may not be amended except in a writing signed by both parties (or, in the case of publisher, by CCC on publisher's behalf).

13. Objection to Contrary Terms: Publisher hereby objects to any terms contained in any purchase order, acknowledgment, check endorsement or other writing prepared by you, which terms are inconsistent with these terms and conditions or CCC's Billing and Payment terms and conditions. These terms and conditions, together with CCC's Billing and Payment terms and conditions (which are incorporated herein), comprise the entire agreement between you and publisher (and CCC) concerning this licensing transaction. In the event of any conflict between your obligations established by these terms and conditions and those established by CCC's Billing and Payment terms and conditions, these terms and conditions shall control.

14. Revocation: Elsevier or Copyright Clearance Center may deny the permissions described in this License at their sole discretion, for any reason or no reason, with a full refund payable to you. Notice of such denial will be made using the contact information provided by you. Failure to receive such notice will not alter or invalidate the denial. In no event will Elsevier or Copyright Clearance Center be responsible or liable for any costs, expenses or damage incurred by you as a result of a denial of your permission request, other than a refund of the amount(s) paid by you to Elsevier and/or Copyright Clearance Center for denied permissions.

LIMITED LICENSE

The following terms and conditions apply only to specific license types:

15. **Translation**: This permission is granted for non-exclusive world **English** rights only unless your license was granted for translation rights. If you licensed translation rights you may only translate this content into the languages you requested. A professional translator must perform all translations and reproduce the content word for word preserving the integrity of the article. If this license is to re-use 1 or 2 figures then permission is granted for non-exclusive world rights in all languages.

16. **Website**: The following terms and conditions apply to electronic reserve and author websites:
Electronic reserve: If licensed material is to be posted to website, the web site is to be password-protected and made available only to bona fide students registered on a relevant course if:
This license was made in connection with a course,
This permission is granted for 1 year only. You may obtain a license for future website posting,
All content posted to the web site must maintain the copyright information line on the bottom of each image,
A hyper-text must be included to the Homepage of the journal from which you are licensing at http://www.sciencedirect.com/science/journal/xxxxx or the Elsevier homepage for books at http://www.elsevier.com , and
Central Storage: This license does not include permission for a scanned version of the material to be stored in a central repository such as that provided by Heron/XanEdu.

Appendix A Continued

17. **Author website** for journals with the following additional clauses:

All content posted to the web site must maintain the copyright information line on the bottom of each image, and
he permission granted is limited to the personal version of your paper. You are not allowed to download and post the published electronic version of your article (whether PDF or HTML, proof or final version), nor may you scan the printed edition to create an electronic version,
A hyper-text must be included to the Homepage of the journal from which you are licensing at http://www.sciencedirect.com/science/journal/xxxxx . As part of our normal production process, you will receive an e-mail notice when your article appears on Elsevier's online service ScienceDirect (www.sciencedirect.com). That e-mail will include the article's Digital Object Identifier (DOI). This number provides the electronic link to the published article and should be included in the posting of your personal version. We ask that you wait until you receive this e-mail and have the DOI to do any posting.
Central Storage: This license does not include permission for a scanned version of the material to be stored in a central repository such as that provided by Heron/XanEdu.

18. **Author website** for books with the following additional clauses:
Authors are permitted to place a brief summary of their work online only.
A hyper-text must be included to the Elsevier homepage at http://www.elsevier.com

All content posted to the web site must maintain the copyright information line on the bottom of each image
You are not allowed to download and post the published electronic version of your chapter, nor may you scan the printed edition to create an electronic version.
Central Storage: This license does not include permission for a scanned version of the material to be stored in a central repository such as that provided by Heron/XanEdu.

19. **Website** (regular and for author): A hyper-text must be included to the Homepage of the journal from which you are licensing at http://www.sciencedirect.com/science/journal/xxxxx. or for books to the Elsevier homepage at http://www.elsevier.com

20. **Thesis/Dissertation**: If your license is for use in a thesis/dissertation your thesis may be submitted to your institution in either print or electronic form. Should your thesis be published commercially, please reapply for permission. These requirements include permission for the Library and Archives of Canada to supply single copies, on demand, of the complete thesis and include permission for UMI to supply single copies, on demand, of the complete thesis. Should your thesis be published commercially, please reapply for permission.

21. **Other Conditions**:

v1.6

If you would like to pay for this license now, please remit this license along with your payment made payable to "COPYRIGHT CLEARANCE CENTER" otherwise you will be invoiced within 48 hours of the license date. Payment should be in the form of a check or money order referencing your account number and this invoice number RLNK500656007. Once you receive your invoice for this order, you may pay your invoice by credit card. Please follow instructions provided at that time.

Make Payment To:
Copyright Clearance Center
Dept 001
P.O. Box 843006
Boston, MA 02284-3006

For suggestions or comments regarding this order, contact RightsLink Customer Support: customercare@copyright.com or +1-877-622-5543 (toll free in the US) or +1-978-646-2777.

Gratis licenses (referencing $0 in the Total field) are free. Please retain this printable license for your reference. No payment is required.